Available online at www.sciencedirect.com
SCIENCE DIRECT®
PHYTOCHEMISTRY
Phytochemistry 66 (2005) 2177–2215
www.elsevier.com/locate/phytochem

Review

# Circular dichroism, a powerful tool for the assessment of absolute configuration of flavonoids

Desmond Slade [a,*], Daneel Ferreira [a,b], Jannie P.J. Marais [a]

[a] *National Center for Natural Products Research, Research Institute of Pharmaceutical Sciences, School of Pharmacy, The University of Mississippi University, MS 38677, USA*
[b] *Department of Pharmacognosy, School of Pharmacy, The University of Mississippi, University, MS 38677, USA*

Received 27 August 2004; received in revised form 24 January 2005
Available online 16 March 2005

**Abstract**

Circular dichroism is a powerful tool for establishing the absolute configuration of flavonoids and proanthocyanidin analogues. It has been utilized to study the configuration of flavanones, dihydroflavonols (3-hydroxyflavanones), flavan-3-ols, flavan-4-ols, flavan-3,4-diols, flavans, isoflavans, isoflavanones, pterocarpans, 6a-hydroxypterocarpans, rotenoids, 12a-hydroxyrotenoids, neoflavonoids, 3,4-dihydro-4-arylcoumarins, 4-arylflavan-3-ols, auronols, homoisoflavanones, proanthocyanidins, and various classes of biflavonoids. Results relevant to the correlation of circular dichroic data and the absolute configuration of the diastereoisomers of some of the above classes of compounds will be discussed.


*Keywords:* Circular dichroism; Absolute configuration; Flavonoids; Flavanones; Dihydroflavonols; 3-Hydroxyflavanones; Flavan-3-ols; Flavan-4-ols; Flavan-3,4-diols; Flavans; Isoflavans; Isoflavanones; Pterocarpans; 6a-Hydroxypterocarpans; Rotenoids; 12a-Hydroxyrotenoids; Neoflavonoids; 3,4-Dihydro-4-arylcoumarins; 4-Arylflavan-3-ols

**Contents**

1. Introduction . . . 2178
2. Flavonoids . . . 2179
3. Flavanones . . . 2179
4. Dihydroflavonols (3-hydroxyflavanones) . . . 2180
5. Flavan-3-ols . . . 2181
   5.1. Introduction . . . 2181
   5.2. The $^1L_b$ transition . . . 2183
   5.3. The $^1L_a$ transition . . . 2185
6. Flavan-4-ols . . . 2185
   6.1. 2,4-*cis*-Flavan-4-ols . . . 2185
   6.2. 2,4-*trans*-Flavan-4-ols . . . 2188
7. Flavan-3,4-diols . . . 2189
   7.1. The $^1L_b$ transition . . . 2189
   7.2. The $^1L_a$ transition . . . 2191

* Corresponding author. Tel.: +1 662 915 5928; fax: +1 662 915 5587.
*E-mail address:* dslade@olemiss.edu (D. Slade).

0031-9422/$ - see front matter © 2005 Elsevier Ltd. All rights reserved.
doi:10.1016/j.phytochem.2005.02.002

8. Flavans . . . 2192
9. Isoflavans . . . 2192
10. Isoflavanones . . . 2194
11. Pterocarpans . . . 2195
11.1. Pterocarpans . . . 2195
11.2. 6a-Hydroxypterocarpans . . . 2199
12. Rotenoids . . . 2201
13. Neoflavonoids . . . 2205
13.1. 3,4-Dihydro-4-arylcoumarins . . . 2205
13.2. 4-Arylflavan-3-ols . . . 2205
14. Conclusion . . . 2211
Acknowledgment . . . 2211
References . . . 2211

## 1. Introduction

Plane or linearly polarized light can be viewed as the vector sum of left and right circularly polarized light of equal amplitude and phase. When an optically active medium is traversed by plane polarized light in the wavelength range in which the chromophore of an optically active molecule absorbs, the plane of polarization is rotated at an angle, $\alpha$, and the optically active matter absorbs the left and right hand circularly polarized light differently. The resulting light is therefore elliptically polarized and the medium exhibits circular dichroism (CD). If $\varepsilon_l$ and $\varepsilon_r$ are the molecular extinction coefficients for the left (l) and right (r) polarized light, respectively, the difference, known as the differential dichroic absorption ($\Delta\varepsilon = \varepsilon_l - \varepsilon_r$), is a measure of the intensity of the CD. Molecular ellipticity $[\Theta]$ is related to $\Delta\varepsilon$ by a simple equation: $[\Theta] = 3300\Delta\varepsilon$. (Velluz et al., 1965).

Any optically active compound will exhibit an optical rotatory dispersion (ORD) curve, which gives the optical activity ($\Phi$) in the function of wavelength ($\lambda$ in nm). If the compound under investigation has no chromophores that absorb in the wavelength range being used, the ORD curve is plain or normal, in other words, the curve does not show any extremum. Anomalous ORD curves, however, exhibit a maximum or a minimum, or both, and are observed when the molecule possesses an absorption band in the region being investigated. These anomalous dispersion effects are known as Cotton effects (CEs) (Crabbé, 1967a).

The ORD and CD methods permit analogous configurational conclusions and the data can be mutually and directly interchanged. The two curves can be mutually derived from each other in good approximation by the Kronig–Kramers transform (Velluz et al., 1965). Although the information obtained by ORD and CD is essentially identical, ORD curves are more complicated than CD curves. Since a maximum or minimum in CD corresponds to two peaks with zero transition in ORD, smaller Cotton effects may be easily obscured by positive or negative effects in the region of a strong Cotton effect.

The chromophores of optically active molecules can be classified into two extreme types, namely, inherently dissymmetric chromophores and inherently symmetric chromophores (Moscowitz, 1961) which are asymmetrically perturbed (Crabbé, 1967a,b). The optical activity of compounds belonging to the first group is inherent in the geometry of the chromophore, e.g. hexahelicene (**1**) (Fig. 1). The optical activity of compounds belonging to the second group is induced in the chromophore by

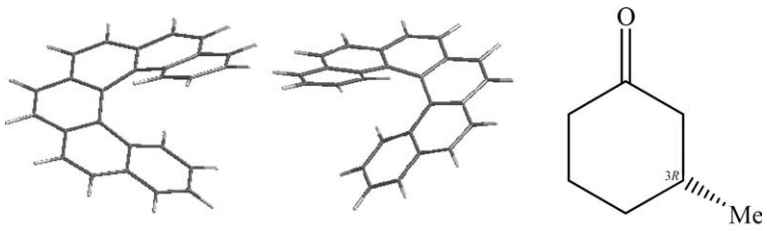


(**1**) (**2**)

Fig. 1. Hexahelicene (**1**) and (*R*)-3-methylcyclohexanone (**2**).

its chiral environment, e.g. (*R*)-3-methylcyclohexanone (**2**) (Fig. 1).

The two main uses of ORD and/or CD in natural product research is for the determination of the absolute configuration and conformation of a molecule.

Chirality sector rules are formulated for various chromophores and are used to determine the absolute configuration if the conformation of a molecule is known or vice versa. The octant rule (Moffitt et al., 1961) for saturated alkyl ketones and aldehydes was the first sector rule used, and along with the exciton chirality rule (Harada and Nakanishi, 1983), remains the most widely known and most successful of the chirality rules. Sector rules focus on chromophores and relate the CD Cotton effect associated with such chromophores to the chirality of the extrachromophoric environment, the chirality of the chromophore, or both (Lightner, 2000).

## 2. Flavonoids

Polyphenols are important secondary metabolites of plants that can be divided into major classes based on their carbon skeleton, e.g. flavonoids and phenolic acids. Flavonoids can be divided into a number of structural classes according to the oxidation state of the C3 unit. A large number of flavonoids are known due to the modification of the C6.C3.C6 skeleton by hydroxylation, methoxylation, glycosylation, other modifications, and combinations thereof (Strack, 1997).

Although the absolute configuration of flavonoids has been elucidated by optical activity and ORD measurements since the early fifties, the more convenient, and in many cases, easier CD method has become more popular since the middle sixties (Djerassi, 1967). CD is now routinely used in the analysis of optically active flavonoids (Lévai, 1998), e.g. flavanones (Gaffield, 1970), dihydroflavonols (Gaffield, 1970; Nonaka et al., 1987; Wu et al., 2003), flavan-3-ols (Korver and Wilkins, 1971; Van Rensburg et al., 1999), flavan-4-ols (Snatzke et al., 1973a), flavan-3,4-diols (Ferreira et al., 2004), flavans (Antus et al., 2001), isoflavans (Versteeg et al., 1999), isoflavanones (Paiva et al., 1994), pterocarpans (Szarvas et al., 2000), 6a-hydroxypterocarpans (Van Aardt et al., 2001), rotenoids (Dewick, 1994), 12a-hydroxyrotenoids (Tahara et al., 1990), neoflavonoids (Nonaka and Nishioka, 1982), 3,4-dihydro-4-arylcoumarins (Fan et al., 1999), 4-arylflavan-3-ols (Van der Westhuizen et al., 1981; Van Zyl et al., 1993), aurones (Bekker et al., 2001), homoisoflavanones (Amschler et al., 1996), proanthocyanidins (Barrett et al., 1979; Botha et al., 1981a; Calzada et al., 1999), and various classes of biflavonoids (Mayer, 2004).

The aim of this review is to demonstrate the utility of CD in the establishment of the absolute configuration and conformation of the biologically important group of flavonoids.

## 3. Flavanones

The flavanones are characterized by two structural features that are important in determining their absolute configuration, namely, the absence of the C2–C3 double bond found in flavones and the presence of the C2 stereocenter. The majority of naturally occurring flavanones have the C2-phenyl group in the α-orientation and is therefore designated as *S*, e.g. (**3**) (Bohm, 1998).

Utilization of CD or ORD in conjunction with NMR spectroscopic data to define the absolute configuration of flavanones was done by Gaffield (1970).

The UV absorptions of flavanones at 270–290 nm (maximum) and 320–330 nm (inflection) have been assigned to the $\pi \rightarrow \pi^*$ and $n \rightarrow \pi^*$ acetophenone chromophore transitions, respectively. The modified octant rule (Snatzke, 1965a), defining the relationship between the chirality of α,β-unsaturated ketones and the sign of their high wavelength CE, was extended to aryl ketones (acetophenones) (Snatzke, 1965b). Thus, flavanones with 2*S* configuration possessing a conformation with *P*-helicity of the heterocyclic ring and having a C2 equatorial aryl group [Figs. 2 and 4(a); Gaffield, 1970] will exhibit a positive CE at the $n \rightarrow \pi^*$ absorption band and a negative CE at the $\pi \rightarrow \pi^*$ absorption band.

The advantage of using the $n \rightarrow \pi^*$ absorption band for configurational assignment is that the sign of this transition is independent on the substitution pattern of the aromatic ring system (Snatzke et al., 1973a), although it must be remembered that the $n \rightarrow \pi^*$ transition at longer wavelength tends to diminish with

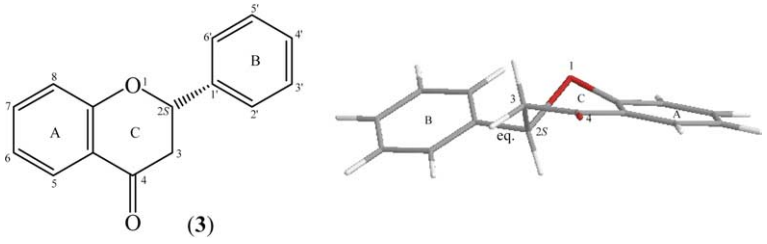


(**3**)

Fig. 2. (2*S*)-flavanones (**3**).

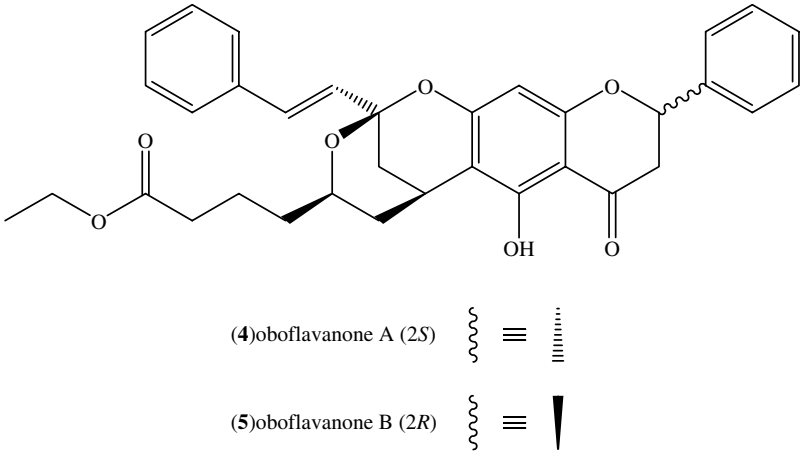


Fig. 3. Oboflavanone A (**4**) and oboflavanone B (**5**).

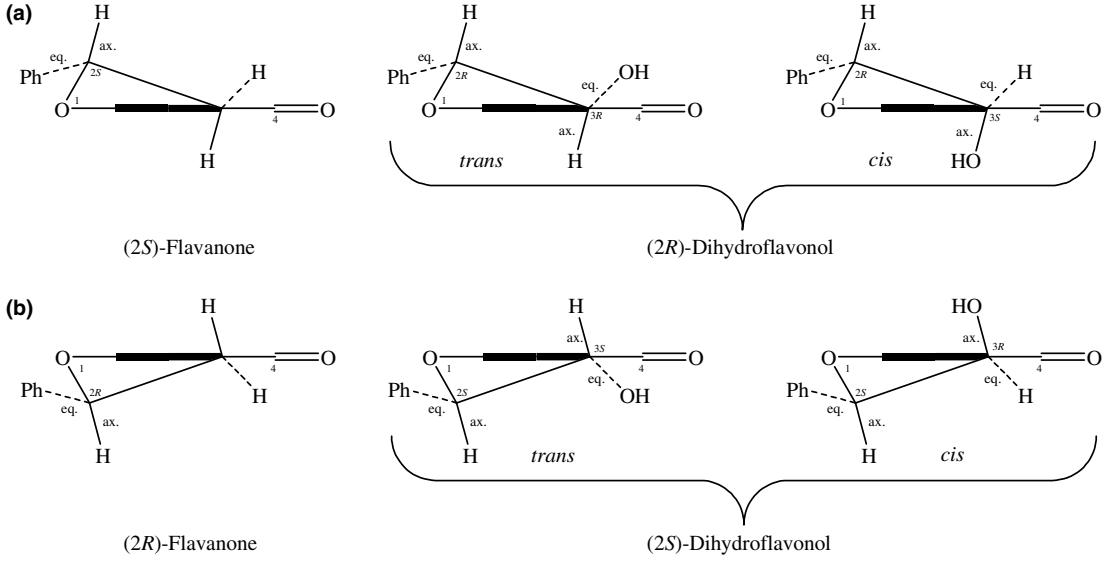


Fig. 4. Hetero-ring conformations (helicities) of the two enantiomeric flavanones and diastereomeric dihydroflavonols with equatorial C2-aryl groups.

increasing amounts of the opposite enantiomers (Gaffield, 1970; Li et al., 2002).

The large coupling constant ($J_{2,3}$) between H2 and H3(ax) of the heterocyclic ring indicates that all natural flavanones are in the thermodynamically favored conformation with the C2-aryl group equatorial (Fig. 2; Clark-Lewis, 1968). This implies that all laevorotatory flavanones possess a 2*S* configuration (Antus et al., 1994; Garo et al., 1998).

A good example of the use of this information can be found in the identification of oboflavanone A (**4**) and oboflavanone B (**5**) (Fig. 3 and Table 1; Dumontet et al., 2004).

Table 1
Configurational assignment at C2 of oboflavanone A (**4**) and oboflavanone B (**5**) using CD data

| Compound | CE (nm) | | | | Configuration at C2 |
|---|---|---|---|---|---|
| | $\pi \rightarrow \pi^*$ | | $n \rightarrow \pi^*$ | | |
| Oboflavanone A (**4**) | 290 | – | 334 | + | (*S*) |
| Oboflavanone B (**5**) | 290 | + | 334 | – | (*R*) |

## 4. Dihydroflavonols (3-hydroxyflavanones)

Dihydroflavonols are intermediates in the biosynthetic pathway to flavonols and anthocyanidins via flavan-3,4-diols. They possess chiral centers at C2 and C3, and therefore have four possible stereoisomers. The (2*R*,3*R*) isomer is the most common in nature,

Table 2
Dihydroflavonol C2 and C3-geometry and configuration

| NMR:$J_{2,3}$ | Result | CE at n → π* (ca. 300–340 nm) | Result | Absolute configuration |
|---|---|---|---|---|
| *trans* | (2*R*,3*R*) or | Positive | 2*R* | (2*R*,3*R*) |
| | (2*S*,3*S*) | Negative | 2*S* | (2*S*,3*S*) |
| *cis* | (2*R*,3*S*) or | Positive | 2*R* | (2*R*,3*S*) |
| | (2*S*,3*R*) | Negative | 2*S* | (2*S*,3*R*) |

but there are cases where all four isomers co-occur (Nonaka et al., 1987; Bohm, 1998).

The assignment of absolute configuration to dihydroflavonols proceeds in two steps. The first step is to identify the relative configuration of the C2 and C3 substituents from NMR coupling constants ($J_{2,3}$) as either *trans* or *cis*. For the *trans*-isomers, the thermodynamically more stable conformation is when H2 and H3 are diaxial and therefore the absolute configuration has to be (2*R*,3*R*) or (2*S*,3*S*). In the *cis* configuration, the thermodynamically more stable conformation is when H2 is axial and H3 is equatorial, and therefore the absolute configuration has to be (2*R*,3*S*) or (2*S*,3*R*). In the second step, CD data is used to determine the absolute configuration at C2. A positive n → π* CE at high wavelength (ca. 300–340 nm) indicates a 2*R* configuration and a negative n → π* CE indicates a 2*S* configuration (Table 2; Gaffield, 1970). As for the flavanones, it should be emphasized that the sign of the n → π* transition depends on the helicity of the heterocyclic ring, which, in conjunction with the relative configuration and the equatorial orientation of the C2-aryl group, establishes the absolute configuration.

It should further be emphasized that (2*R*,3*R*)-dihydroflavonols and (2*S*)-flavanones are homochiral due to a change in the Cahn–Ingold–Prelog priority when going from H at C3 in the flavanones to OH in the dihydroflavonols. The fact that (2*R*,3*R*)-dihydroflavonols and (2*S*)-flavanones indeed have the same hetero-ring helicities and thus similar signs of their n → π* transition CEs is demonstrated in Fig. 4.

Table 3
Configurational assignment at C2 and C3 of phellodensin-A (**6**) and phellodensin-C (**7**) using $^1$H NMR and CD data

| Compound | NMR:$J_{2,3}$ | CE at n → π* (ca. 300 and 340 nm) | Absolute configuration |
|---|---|---|---|
| Phellodensin A (**6**) | *trans* | Positive | (2*R*,3*R*) |
| Phellodensin C (**7**) | *trans* | Positive | (2*R*,3*R*) |

The CEs due to the positive n → π* transitions in their CD spectra were used in the determination of the absolute configuration of phellodensin-A (**6**) and phellodensin-C (**7**) (Fig. 5 and Table 3; Wu et al., 2003) as both being (2*R*,3*R*).

## 5. Flavan-3-ols

### 5.1. Introduction

The chroman chromophore (**8**) (Fig. 6) is present in various naturally occurring *O*-heterocycles. The chroman derivatives belong to the benzene chromophores with a chiral second sphere. The achiral benzene A-ring chromophore is chirally perturbed by the fused chiral *O*-heterocyclic ring (second sphere) and the substituents of the heterocyclic ring (third sphere). This gives rise to the observed CEs at ca. 260–280 nm ($^1L_b$ band) and ca. 200–240 nm ($^1L_a$ band). The chirality (conformation) of the heterocyclic ring can be deduced from the CD spectrum if the relationship between the helicity of the nonaromatic ring and the sign of the $^1L_b$ band CD is known. The absolute configuration can then be assigned from NMR spectroscopic experiments that give the relative configuration between the substituents at the chiral centers.

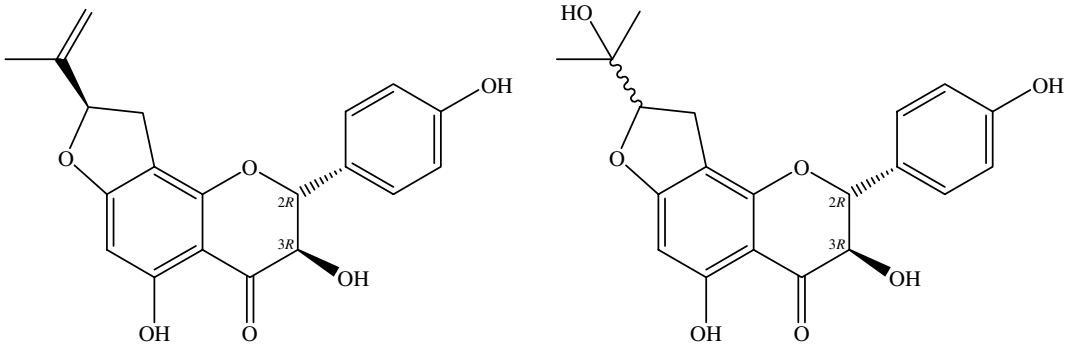


(**6**) phellodensin-A (**7**) phellodensin-C

Fig. 5. Phellodensin-A (**6**) and phellodensin-C (**7**).

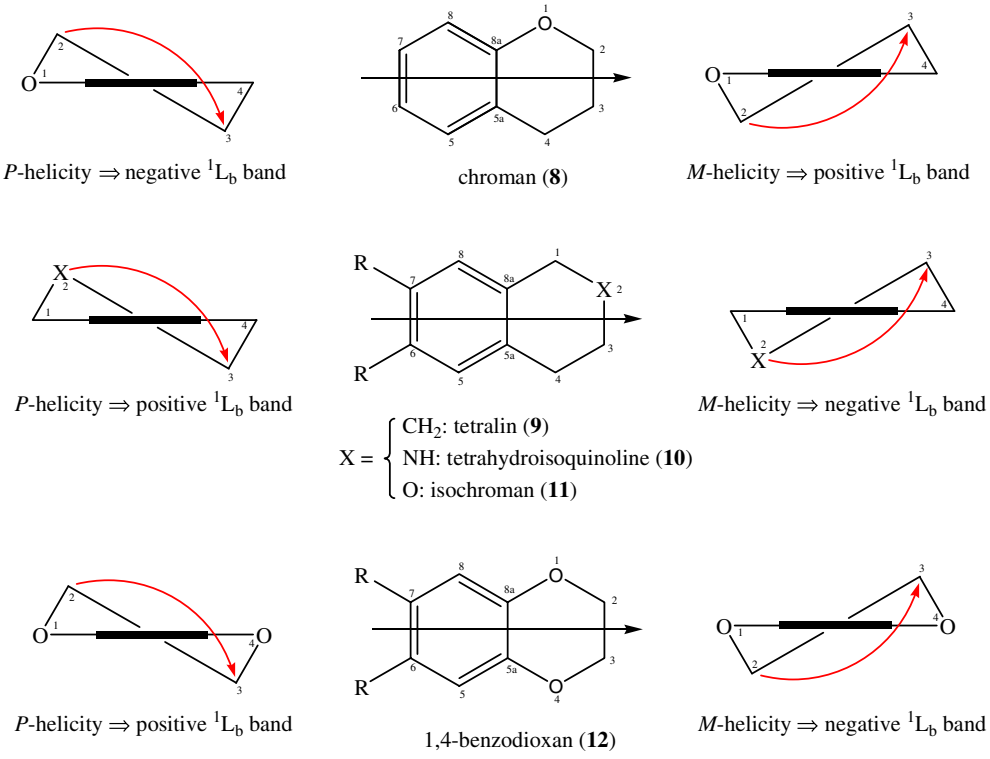


Fig. 6. Helicity rule or sign of the second sphere contribution to the $^1L_b$ band CD. The arrow (black) indicates the direction of projection. R=H or *O*-alkyl.

A helicity rule for the benzene chromophore of chiral tetralin (**9**), tetrahydroisoquinoline (**10**) (Snatzke and Ho, 1971), isochroman (**11**) (Antus et al., 1983) and 1,4-benzodioxan (**12**) (Antus et al., 1991) derivatives was developed and can be formulated as follows: if there is no pseudoaxial substituent at the benzylic C4 and the benzene A-ring is not further substituted, *P*-helicity of the hetero-ring (half-chair conformation) leads to a positive and *M*-helicity to a negative CE within the $^1L_b$ band (Fig. 6). Sector rules were developed for third sphere contributions, namely, the nonaromatic ring substituents (Luche et al., 1972; Dornhege and Snatzke, 1970; Schulte and Snatzke, 1989; Hagishita and Kuriyama, 1982).

In homochiral compounds the signs of the second and third sphere contributions to the $^1L_b$ band CE depend on the substitution pattern of the benzene ring (Snatzke et al., 1972, 1973b). The "spectroscopic moments" ($q$) of different achiral substituents, whose signs and magnitudes have been investigated (Platt, 1949, 1951; Petruska, 1961), can be used to explain the change in sign of the $^1L_b$ band CE together with the electric transition moment vector ($\mu = \Sigma q$), which is the sum of the spectroscopic moments (Fig. 7).

It is therefore clear that as a first step it has to be determined which form of Snatzke's helicity rule is valid for these chromophores, and since the benzene rings are substituted in most of these natural products, the influence of the achiral substituents on the chiroptical properties also has to be determined for each chromophore to apply their CD correctly for configurational assignment.

Antus et al. (2001) reported that methoxy and/or hydroxyl groups at C2, C3, C5 and/or C7 do not change the chroman helicity rule, so that substituted chroman derivatives can also be analyzed using this technique.

Simple aromatic compounds usually show three major electronic transitions: two strong absorption bands at ca. 180–190 and 200–240 nm, and a weak transition, usually showing considerable fine structure, at ca. 260–280 nm (Table 4). The weak $^1L_b$ transition at ca. 260–280 nm is formally forbidden in symmetrical aromatic compounds, but in any dissymmetric aromatic system, the $\pi \rightarrow \pi^*$ transition will become optically active (Crabbé, 1967b).

Flavan-3-ols (catechins), e.g. (**17**), have two aromatic chromophores, namely, the benzene A- and B-rings, with the absorption bands of these chromophores found at ca. 280 nm ($^1L_b$ transition) and ca. 240 nm ($^1L_a$ transition). The presence of two aromatic chromophores gives two bands in each region (Korver and Wilkins, 1971). The flavan-3-ols have two stereocenters and therefore four possible diastereomers, namely, (2*R*,3*S*)-2,3-*trans*, (2*S*,3*R*)-2,3-*trans*, (2*R*,3*R*)-2,3-*cis*, and

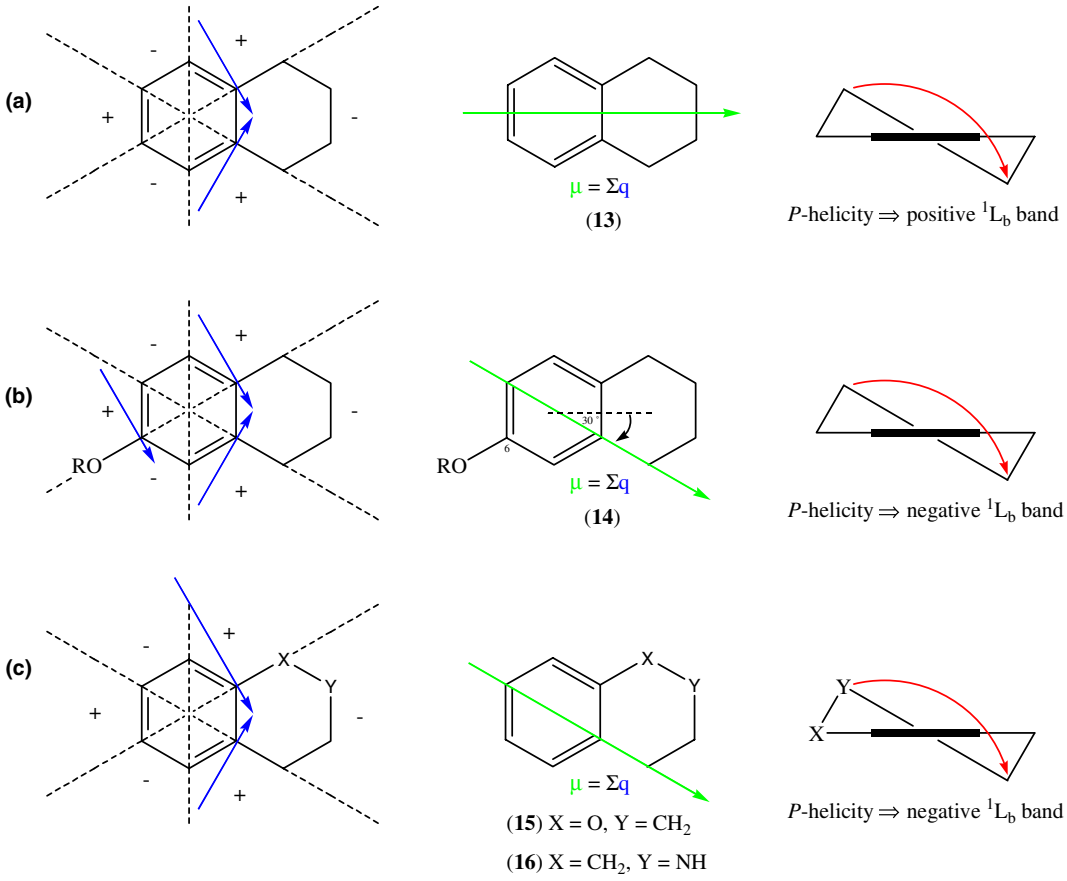


Fig. 7. Platt polarization diagrams for the $^1L_b$ band. The small (blue) arrows are the spectroscopic moment vectors ($q$) and the bigger (green) arrows are the electric transition moment vectors ($\mu$), namely, the translation of the electron charge during the transition. (a) Tetralins (**13**) having no substituent on the aromatic ring, (b) 6-substituted tetralins (**14**) (R=H or alkyl), and (c) chroman (**15**) (X=O, Y=$CH_2$) and tetrahydroisoquinoline (**16**) (X=$CH_2$, Y=NH) chromophores without substituents on the aromatic ring.

Table 4
The first three UV absorption bands of aromatic systems

| Wavelength (nm) | Band |
|---|---|
| 260–280 | α<br>$^1L_b$<br>$^1A_{1g} \rightarrow {}^1B_{2u}$<br>$^1A \rightarrow {}^1L_b$<br>B |
| 200–240 | *p*<br>$^1L_a$<br>$^1A_{1g} \rightarrow {}^1B_{1u}$<br>$^1A \rightarrow {}^1L_a$<br>$E_2$ |
| 180–190 | β<br>$^1B_a$<br>$^1A_{1g} \rightarrow {}^1E_{1u}$<br>$^1A \rightarrow {}^1B$<br>$E_1$ |

(2*S*,3*S*)-2,3-*cis* exist. According to Snatzke et al. (1973b), the A-ring chromophore forms the first sphere, the heterocyclic C-ring forms the second sphere, and the B-ring chromophore and the C3-substituent form the third sphere.

### 5.2. The $^1L_b$ transition

The C-ring (second sphere) of flavan-3-ols (**17**) is the closest chiral sphere to the A-ring chromophore (first sphere), and therefore determines not only the sign of the CE within each absorption band, but also a significant part of the magnitude. The sign of the CE of the aromatic A-ring is determined by the chirality of the heterocyclic C-ring, with the absolute configuration at C3 having only a minor influence, which is similar to the situation found for tetralins (Dornhege and Snatzke, 1970). The chirality of the C-ring is determined by the preference of the C2-aryl B-ring for an equatorial position as established by NMR spectroscopic analysis (Fig. 8; Clark-Lewis, 1968).

The CD spectra of flavan-3-ols (**17**) should therefore be explicable in terms of the helicity rules proposed for the chroman (3,4-dihydro-2*H*-pyran) ring system.

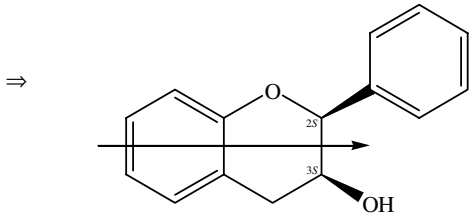


(**17**)

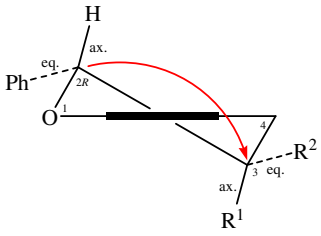


**E-conformer**

*P*-helicity ⇒ negative $^1L_b$ band

$R^1$ = OH, $R^2$ = H: (2*R*,3*R*)-2,3-*cis*

$R^1$ = H, $R^2$ = OH: (2*R*,3*S*)-2,3-*trans*

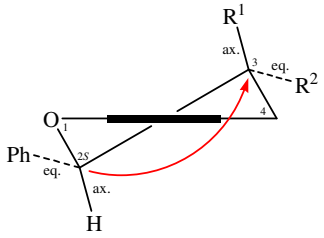


**E-conformer**

*M*-helicity ⇒ positive $^1L_b$ band

$R^1$ = OH, $R^2$ = H: (2*S*,3*S*)-2,3-*cis*

$R^1$ = H, $R^2$ = OH: (2*S*,3*R*)-2,3-*trans*

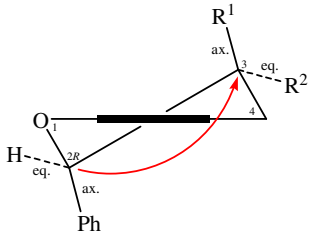


**A-conformer**

*M*-helicity ⇒ positive $^1L_b$ band

$R^1$ = H, $R^2$ = OH: (2*R*,3*R*)-2,3-*cis*

$R^1$ = OH, $R^2$ = H: (2*R*,3*S*)-2,3-*trans*

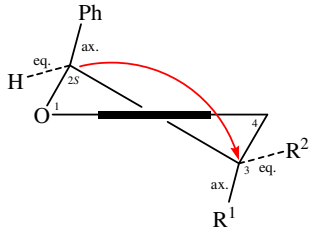


**A-conformer**

*P*-helicity ⇒ negative $^1L_b$ band

$R^1$ = H, $R^2$ = OH: (2*S*,3*S*)-2,3-*cis*

$R^1$ = OH, $R^2$ = H: (2*S*,3*R*)-2,3-*trans*

Fig. 8. *P*- and *M*-helicity of the chroman C-ring of flavan-3-ols (**17**). Projection is in the direction of the arrow. The wedge represents the plane of the benzenoid A-ring.

*P*-helicity of the C-ring with its preferred half-chair/C2-sofa conformation (Porter et al., 1986) should lead to positive CEs within the $^1L_b$ transition, and *M*-helicity to negative CEs (Snatzke et al., 1973b) as was recorded for a series of tetralin derivatives (Dornhege and Snatzke, 1970). Flavan-3-ols with 2*R* and 2*S* absolute configuration, respectively, display *P*- and *M*-helicity, respectively (Fig. 8).

However, CD data (Korver and Wilkins, 1971; Van Rensburg et al., 1999) indicates that 2*R* and 2*S* absolute configurations give rise to negative and positive CEs, respectively, for chromophore A in the $^1L_b$ region (Figs. 9 and 10; Table 5). This result is opposite to that found for the tetralins, which conforms to the helicity rules. A possible reason for this might be the loss of $C_{2v}$ symmetry in going from the tetralin to the chroman chromo-

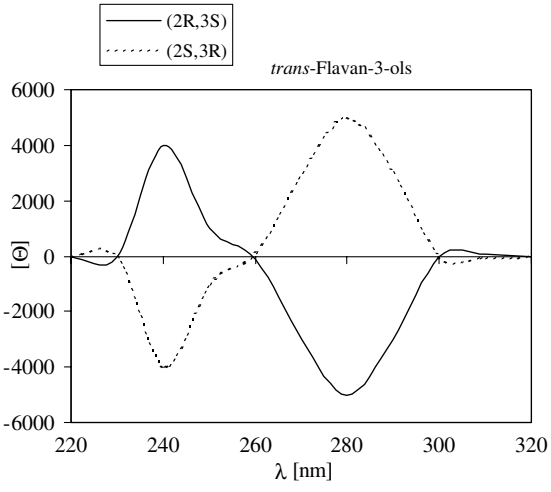


Fig. 9. CD spectra of *trans*-flavan-3-ols.

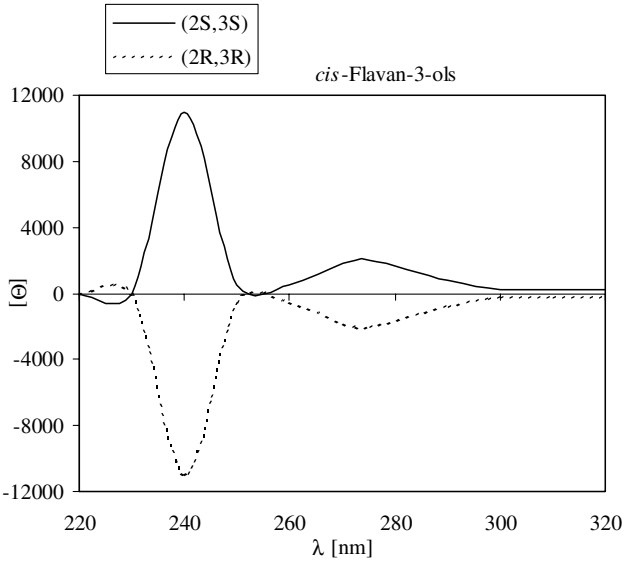


Fig. 10. CD spectra of *cis*-flavan-3-ols.

Table 5
Flavan-3-ol C2- and C3-geometry and configuration

| CE at $^1L_b$ (ca. 280 nm) | Result | Helicity | NMR:$J_{2,3}$ | Absolute configuration |
|---|---|---|---|---|
| Negative | 2*R* | *P* | *trans* | (2*R*,3*S*) |
| | | | *cis* | (2*R*,3*R*) |
| Positive | 2*S* | *M* | *trans* | (2*S*,3*R*) |
| | | | *cis* | (2*S*,3*S*) |

phore. An n → π* transition from the $p_z$-orbital of the C-ring oxygen to the π*-orbital of the A-ring might also contribute to the inversion of the rule (Korver and Wilkins, 1971).

The A-conformation for 2,3-*cis*-flavan-3-ols is a relatively stable conformation which leads to a reduced amplitude of the long wavelength CE due to the inversion of helicity in going from an E- to an A-conformation (Figs. 8 and 10; Van Rensburg et al., 1999).

Table 6
Flavan-3-ol CEs

| Absolute configuration | NMR:$J_{2,3}$ | Helicity | CE $^1L_a$ (ca. 240 nm) | CE at $^1L_b$ (ca. 280 nm) |
|---|---|---|---|---|
| (2*R*,3*S*) | *trans* | *P* | Positive | Negative |
| (2*R*,3*R*) | *cis* | *P* | Negative | Negative |
| (2*S*,3*R*) | *trans* | *M* | Negative | Positive |
| (2*S*,3*S*) | *cis* | *M* | Positive | Positive |

### 5.3. The $^1L_a$ transition

The (2*R*,3*S*)- and (2*S*,3*R*)-*trans* enantiomers have CEs of opposite sign and the (2*R*,3*R*)- and (2*S*,3*S*)-*cis* enantiomers have CEs of the same sign for the $^1L_a$ transition (ca. 240 nm) as compared to the $^1L_b$ transition (ca. 280 nm). Positive and negative CEs in the 240 nm region seem to indicate 3*S* and 3*R* absolute configurations, respectively (Table 6; Figs. 9 and 10). Exceptions to this rule occur when the A-ring is devoid of hydroxylation (Van Rensburg et al., 1999).

A new flavan-3-ol glucoside was isolated from barley (*Hordeum vulgare* L.) and identified as (2*R*,3*S*)-catechin-7-*O*-β-D-glucopyranoside (**18**) using NMR, FAB-MS, UV and CD. A $J_{2,3}$ coupling constant of 7.4 Hz confirmed a 2,3-*trans* configuration and a negative CE at 280 nm indicated a 2*R* configuration (Fig. 11; Friedrich and Galensa, 2002).

## 6. Flavan-4-ols

### 6.1. 2,4-cis-Flavan-4-ols

The NMR spectra and respective $J_{2,4}$ coupling constants of (+)-(2*R*,4*R*)-4-aminoflavan hydrochloride (**19**), (+)-(2*R*,4*R*)-4-acetamidoflavan (**20**) (Bognár et al., 1970), and (2*R*,4*R*)-flavan-4-ol benzoate (**21**) (Bolger et al., 1966) established their relative configurations as *cis* (Fig. 12) with the dihydropyran C-ring having either a half-chair or a sofa conformation.

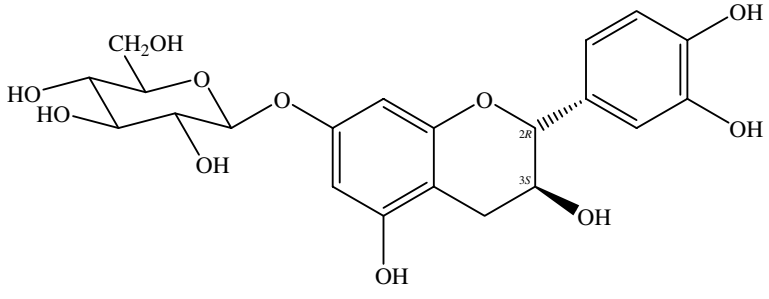


(**18**)

Fig. 11. (2*R*,3*S*)-catechin-7-*O*-β-D-glucopyranoside (**18**).

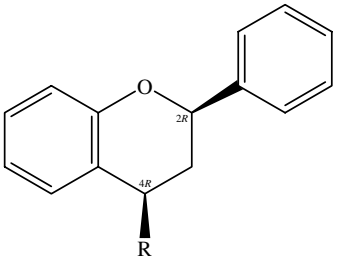


R = { $NH_2$·HCl: (+)-(2*R*,4*R*)-4-aminoflavan hydrochloride (**19**)
NHAc: (+)-(2*R*,4*R*)-4-acetamidoflavan (**20**)
OBz: (2*R*,4*R*)-flavan-4-ol benzoate (**21**)

Fig. 12. (2*R*,4*R*)-*cis*-flavans (**19**–**21**).

With a half-chair conformation of the C-ring (Fig. 13), C4–OH would be forced into the unfavorable $\psi$-equatorial (pseudo-equatorial) position (H2 and H4 diaxial), while in the other possible half-chair conformation, the C2-phenyl group has to adopt the equally unfavorable axial position (H2 and H4 diequatorial). The boat conformation can also be discarded by conformational analysis. In the sofa conformation, C4–OH is oriented in such a way that *peri*-interaction is avoided, and therefore the sofa conformation seems more probable than the half-chair conformation (Fig. 14; Snatzke et al., 1973a).

The CE of tetralins and tetrahydroisoquinolines can be interpreted by differentiating between second- and third-sphere contributions, the former generally being stronger than the latter (Dornhege and Snatzke, 1970; Barry et al., 1971; Luche et al., 1972; Snatzke and Ho, 1971; Snatzke et al., 1972). Tetralin and tetrahydroisoquinoline derivatives without A-ring substitution have positive CEs for both the $^1L_a$ and $^1L_b$ transitions if the chiral C-ring has *P*-helicity. For derivatives with A-ring substitution, the same rule may apply, or the inverse may hold, depending on the substitution pattern.

Flavonoids, in contrast to the tetralins and tetrahydroisoquinolines that use two carbons, utilize one

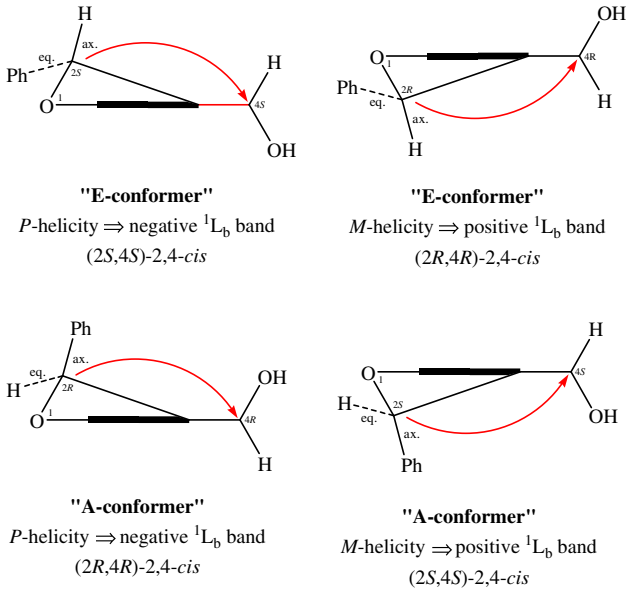


Fig. 14. Sofa conformations for 2,4-*cis*-flavan-4-ols.

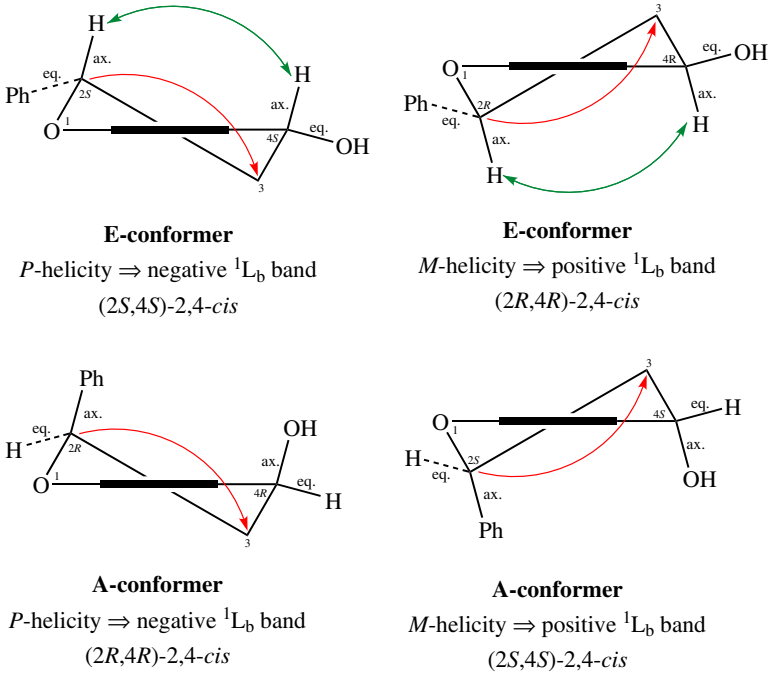


Fig. 13. Half-chair conformations for 2,4-*cis*-flavan-4-ols. The green arrows indicate *peri*-interactions.

oxygen and one carbon to connect the chiral C-ring to the benzene A-ring. Also, with a sofa conformation, the chirality of the second sphere is no longer as strong as for tetralins and tetrahydroisoquinolines with their half-chair conformations. The second-sphere contributions of the CE will thus be smaller, and with the chiral C4–OH next to the A-ring chromophore, third-sphere contributions may become even stronger (Snatzke et al., 1973a).

The (2*R*,4*R*)-*cis* diastereomer is expected to have a negative second-sphere contribution for the chroman (A-ring) chromophore when the sofa conformation is assumed (Fig. 14). The contribution of the C-ring chromophore, which depends strongly on its preferred conformation, to the CD is expected to be one or two orders of magnitude smaller, although it can still contribute like any other substituent to the third-sphere effects for the A-ring chromophore.

It was experimentally found that epimerization at C4 changes the sign of the $^1L_b$ band and therefore it can be assumed that $C_2$ is a good approximation for the symmetry of the chroman molecule and that the plane of the benzene A-ring is a nodal plane. The (2*R*,4*R*)-*cis* diastereomer (**22**) is expected to have a positive contribution from C4–OH for the CEs in both the $^1L_a$ and $^1L_b$ bands (Fig. 15). For the $^1L_b$ band and with a sofa conformation of the chiral ring, the influence of the second-sphere is much smaller than that of the C4–OH group next to the A-ring chromophore, i.e., the third-sphere contribution (Snatzke et al., 1973a).

Although the second-sphere contributions are smaller than that of the third-sphere, the helicity rule for the *cis*-enantiomers is the same as that for the flavan-3-ols (Tables 6 and 7) and inverse to the rule for the tetralins.

Antus et al. (2001) treated the 2,4-*cis* enantiomers as having a half-chair conformation (Fig. 13) with their helicity governed by the equatorial orientation of the C2-phenyl group, but came to the same conclusion: *P*-/*M*-helicity of the *O*-heterocyclic ring in the chroman chromophore is reflected by a negative/positive CE within the $^1L_b$ band transition of the benzene ring when the *O*-heterocyclic ring adopts a half-chair conformation and there is no substituent on the fused aromatic ring (Table 7).

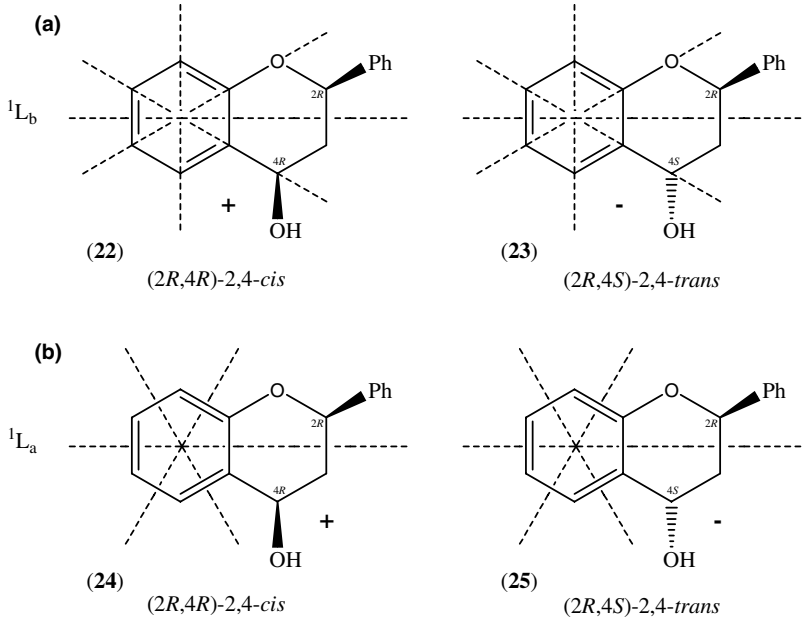


Fig. 15. Sector rule for third-sphere contributions to the (a) $^1L_b$ (**22**–**23**) and (b) $^1L_a$ bands (**24**–**25**).

Table 7
Flavan-4-ol CEs

| Absolute configuration | NMR:$J_{2,4}$ | Helicity | CE $^1L_a$ (ca. 240 nm) | CE at $^1L_b$ (ca. 280 nm) |
|---|---|---|---|---|
| (2*R*,4*R*) | *cis* | *M* | Positive | Positive |
| (2*S*,4*S*) | *cis* | *P* | Negative | Negative |
| (2*R*,4*S*) | *trans* | *M* | Negative | Negative |
| (2*S*,4*R*) | *trans* | *P* | Positive | Positive |

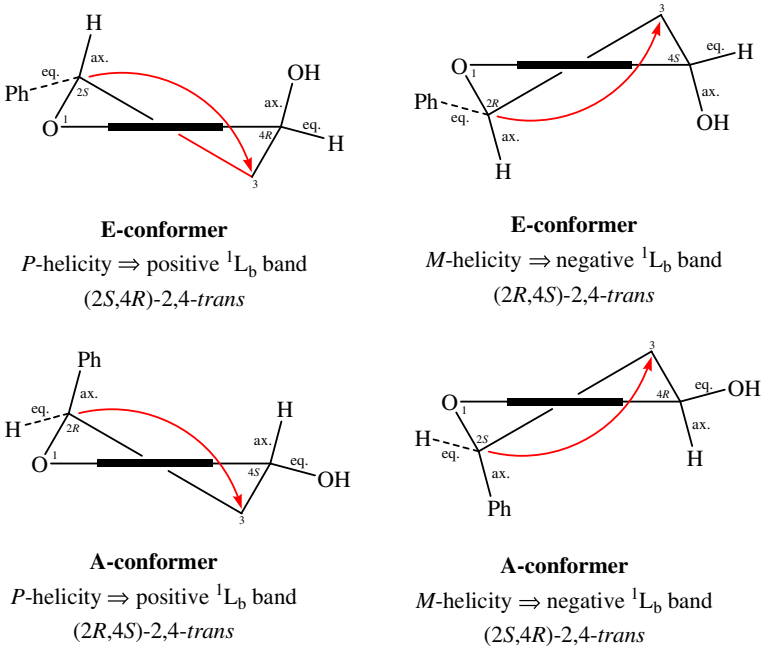


Fig. 16. Half-chair conformations for 2,4-*trans*-flavan-4-ols.

### 6.2. 2,4-trans-Flavan-4-ols

NMR spectroscopic analysis indicates that 2,4-*trans*-flavan-4-ols have either a half-chair (Fig. 16) or a sofa conformation (Fig. 17); conformational analysis cannot differentiate between these two forms. Second-sphere helicity and third-sphere contribution of the C4–OH group for the (2*R*,4*S*)-2,4-*trans* enantiomers (**23/25**) (Fig. 15) are both predicted to show negative CEs in the $^1L_a$ and $^1L_b$ bands for the half-chair and the sofa conformation. The absolute value of the rotational strength of the more reliably measurable $^1L_b$ band is practically the same for the two epimers (2*R*,4*R*)-2,4-*cis*-flavan-4-ol (**22/24**) and (2*R*,4*S*)-2,4-*trans*-flavan-4-ol (**23/25**). It can therefore be concluded that the dihydropyran C-ring of the *trans*-compounds prefers the sofa conformation with C2 out of the plane of the benzene A-ring, although the half-chair conformation could not be excluded totally (Snatzke et al., 1973a).

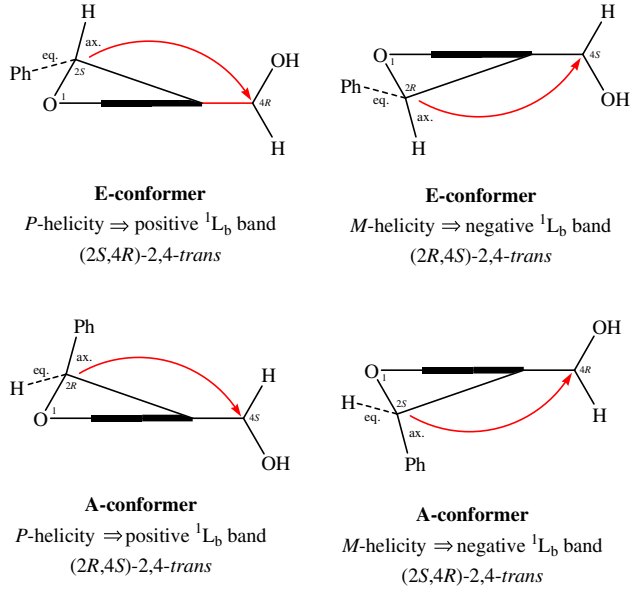


Fig. 17. Sofa conformations for 2,4-*trans*-flavan-4-ols.

Antus et al. (2001) concluded that the 2,4-*trans*-flavan-4-ols follows a different rule to that of the 2,4-*cis*-flavan-4-ols (half-chair/sofa conformation) (Figs. 13 and 14) due to the axial C4–OH that forces the *O*-heterocyclic ring into a flat sofa conformation (Fig. 17) which makes the chiral third-sphere (substituent at C4) contribution overrule the second one (helicity of the *O*-heterocyclic ring). Thus, *P*-/*M*-helicity is reflected by a positive/negative CE within the $^1L_b$ band transition of the benzene ring when the *O*-heterocyclic ring adopts a sofa conformation and there is no substituent on the fused aromatic ring (Fig. 17 and Table 7).

The CD data for three flavan-4-ols is tabulated in Table 8 (Fig. 15; Snatzke et al., 1973a).

Table 8
CD spectra data of flavan-4-ols. Solvent: acetonitrile

| Flavan-4-ol | $\lambda_{max}(\Delta\varepsilon)$ |
|---|---|
| (2*R*,4*R*)-*cis* | 283 (+1.22), 276 (+1.28), 227 (+2.23) |
| (2*R*,4*S*)-*trans* | 282 (−1.17), 276 (−1.17), 226 (−7.62) |
| (2*S*,4*R*)-*trans* | 282 (+1.44), 276 (+1.41), 226 (+0.80) |

## 7. Flavan-3,4-diols

The flavan-3,4-diols and flavan-3-ols are the biogenetic precursors to the proanthocyanidins (condensed tannins) (Ferreira et al., 1999). The majority of flavan-3,4-diols have been isolated from the bark or wood of *Acacia* species (Haslam, 1982).

The relative configuration of flavan-3,4-diols (**26**) is readily accessable from the $^{3}J_{H,H}$ values of their C-ring three-bond proton coupling constants (Clark-Lewis et al., 1964). Small but significant differences in the coupling constants of 2,3-*cis*-3,4-*trans* and 2,3-*cis*-3,4-*cis* analogues allow assignment of the relative configurations via appropriate NOE experiments.

### 7.1. The $^{1}L_{b}$ transition

The $^{1}L_{b}$ band of C-ring substituted flavans at ca. 280 nm is usually exploited for configurational assignment since it is less prone to mixing with other transitions or overlapping than the $^{1}L_{a}$ band at shorter wavelengths (Antus et al., 2001). The sign and a substantial part of the magnitude of the CE within each

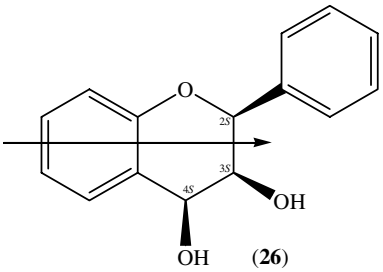


(**26**)

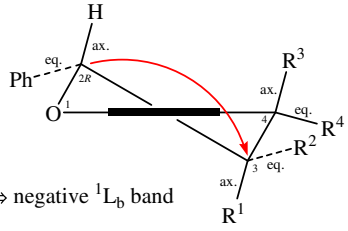


*P*-helicity ⇒ negative $^{1}L_{b}$ band

| C2/C3 | C3/C4 | C2 | C3 | C4 | $R^1$ | $R^2$ | $R^3$ | $R^4$ | Helicity |
|---|---|---|---|---|---|---|---|---|---|
| *cis* | *cis* | *R* | *R* | *R* | OH | H | H | OH | *P* |
| *trans* | *trans* | *R* | *S* | *R* | H | OH | H | OH | *P* |
| *cis* | *trans* | *R* | *R* | *S* | OH | H | OH | H | *P* |
| *trans* | *cis* | *R* | *S* | *S* | H | OH | OH | H | *P* |

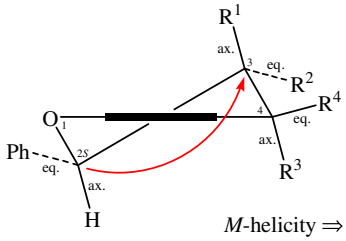


*M*-helicity ⇒ positive $^{1}L_{b}$ band

| C2/C3 | C3/C4 | C2 | C3 | C4 | $R^1$ | $R^2$ | $R^3$ | $R^4$ | Helicity |
|---|---|---|---|---|---|---|---|---|---|
| *cis* | *cis* | *S* | *S* | *S* | OH | H | H | OH | *M* |
| *trans* | *trans* | *S* | *R* | *S* | H | OH | H | OH | *M* |
| *cis* | *trans* | *S* | *S* | *R* | OH | H | OH | H | *M* |
| *trans* | *cis* | *S* | *R* | *R* | H | OH | OH | H | *M* |

Fig. 18. Half-chair conformations for flavan-3,4-diols (**26**).

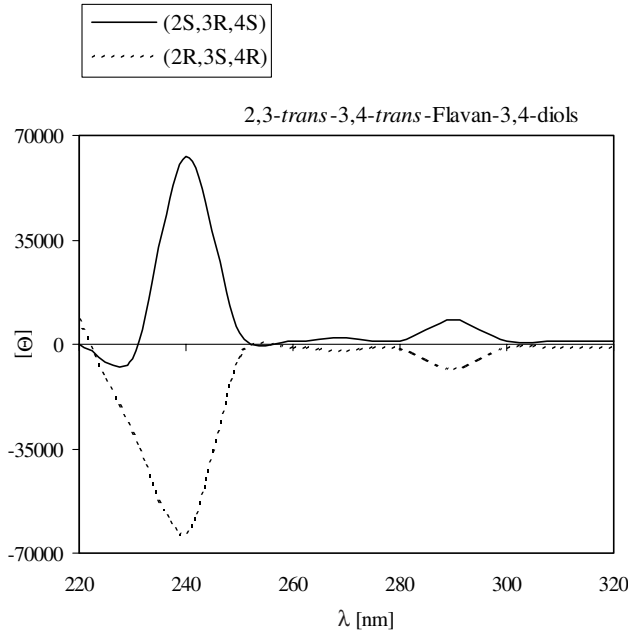


Fig. 19. CD spectra of 2,3-*trans*-3,4-*trans*-flavan-3,4-diols.

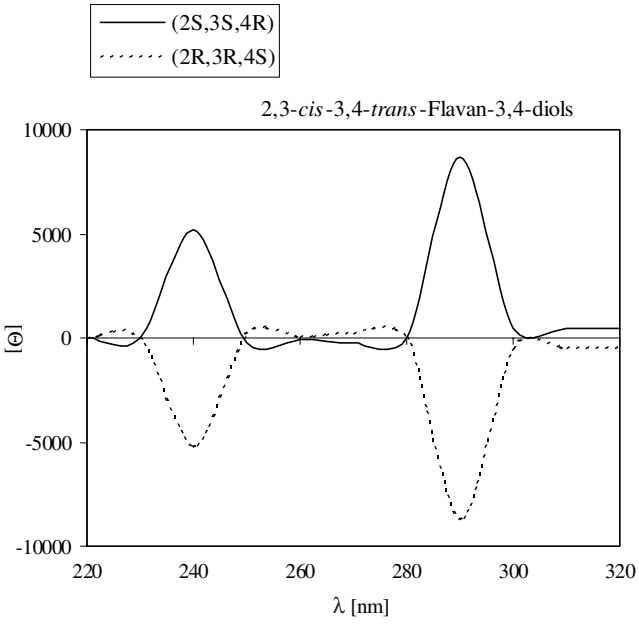


Fig. 20. CD spectra of 2,3-*cis*-3,4-*trans*-flavan-3,4-diols.

absorption band are determined by the chiral sphere closest to the A-ring chromophore, i.e., the C-ring of the flavan-3,4-diols. Accordingly, the absolute configuration at C3 will have a minor influence on the sign of the CE of this transition. Thus, the spectra of flavan-3,4-diols with their chiral second-sphere (C-ring) and the preference of the B-ring for an equatorial orientation, should be explicable in terms of the "inversed" helicity rules proposed for the dihydropyran ring system (Korver and Wilkins, 1971; Nel et al., 1999; Van Rensburg et al., 1999; Snatzke et al., 1973a; Majer et al., 1995; Antus et al., 2001). *P*-Helicity (2*R* configuration) of the C-ring with its preferred half-chair/C2-sofa conformation (Clark-Lewis et al., 1964; Porter et al., 1986) should lead to negative CEs within the $^1L_b$ transition, and *M*-helicity (2*S* configuration) to positive ones (Figs. 18–20; Table 9).

The E-conformer of the all-*trans* analogues, namely, (2*R*,3*S*,4*R*)- and (2*S*,3*R*,4*S*)-2,3-*trans*-3,4-*trans*-flavan-3,4-diol, experiences allylic strain between C4–OH and H5. This results in a conformational change to alleviate the strain and leads to a relatively stable inversed half-chair/C2 sofa A-conformation (Porter et al., 1986) with *M*- as opposed to *P*-helicity for the 2*R*-all-*trans*-flavan-3,4-diols, and vice versa for the 2*S* analogues (Fig. 21). The net effect of the conformational change is a reduced amplitude of the $^1L_b$ CE for the all-*trans* analogues compared to, e.g., the 2,3-*trans*-3,4-*cis* analogues.

The A-conformer of the 2,4-*cis*-diaxial analogues, namely, (2*R*,3*R*,4*R*)- and (2*S*,3*S*,4*S*)-2,3-*cis*-3,4-*cis*-flavan-3,4-diol, and (2*R*,3*S*,4*R*)- and (2*S*,3*R*,4*S*)-2,3-*trans*-3,4-*trans*-flavan-3,4-diol, may be stabilized via hydrogen bonding between C4–OH and the aromatic B-ring (Fig. 22). Once C4–OH is derivatized, hydrogen bonding and hence stabilization of an A-conformer are eliminated and the amplitude of the $^1L_b$ band CE increases relative to that of the $^1L_a$ transition (Ferreira et al., 2004).

The E-conformer of the all-*cis* analogues, namely, (2*R*,3*R*,4*R*)- and (2*S*,3*S*,4*S*)-2,3-*cis*-3,4-*cis*-flavan-3,4-diol, is stabilized by hydrogen bonding between the axial C3–OH and the *O*-heteroatom of the C-ring (Fig. 23; Clark-Lewis and Williams, 1967).

Table 9
Flavan-3,4-diol CEs

| CE at $^1L_b$ (ca. 280 nm) | Helicity | C2 | NMR:$J_{2,3}$ | C3 | NMR:$J_{3,4}$ | C4 | Absolute configuration |
|---|---|---|---|---|---|---|---|
| Positive | *M* | *S* | *cis* | *S* | *cis* | 4*S* | 2*S*,3*S*,4*S* |
| | | | | | *trans* | 4*R* | 2*S*,3*S*,4*R* |
| | | | *trans* | *R* | *cis* | 4*R* | 2*S*,3*R*,4*R* |
| | | | | | *trans* | 4*S* | 2*S*,3*R*,4*S* |
| Negative | *P* | *R* | *cis* | *R* | *cis* | 4*R* | 2*R*,3*R*,4*R* |
| | | | | | *trans* | *4S* | *2R,3R,4S* |
| | | | *trans* | *S* | *cis* | 4*S* | 2*R*,3*S*,4*S* |
| | | | | | *trans* | 4*R* | 2*R*,3*S*,4*R* |

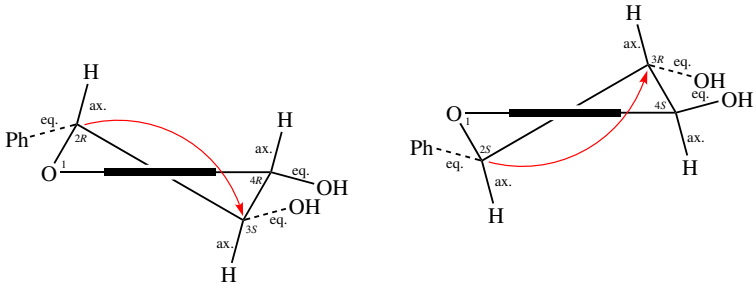

**E-conformer**

*P*-helicity ⇒ negative $^1L_b$ band

(2*R*,3*S*,4*R*)-2,3-*trans*-3,4-*trans*

**E-conformer**

*M*-helicity ⇒ positive $^1L_b$ band

(2*S*,3*R*,4*S*)-2,3-*trans*-3,4-*trans*

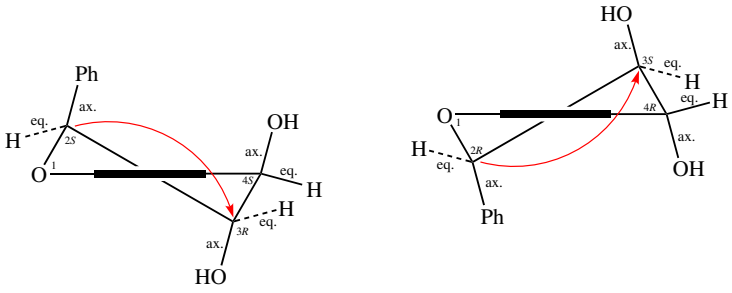

**A-conformer**

*P*-helicity ⇒ negative $^1L_b$ band

(2*S*,3*R*,4*S*)-2,3-*trans*-3,4-*trans*

**A-conformer**

*M*-helicity ⇒ positive $^1L_b$ band

(2*R*,3*S*,4*R*)-2,3-*trans*-3,4-*trans*

Fig. 21. A-conformer half-chair conformations for all-*trans*-flavan-3,4-diols.

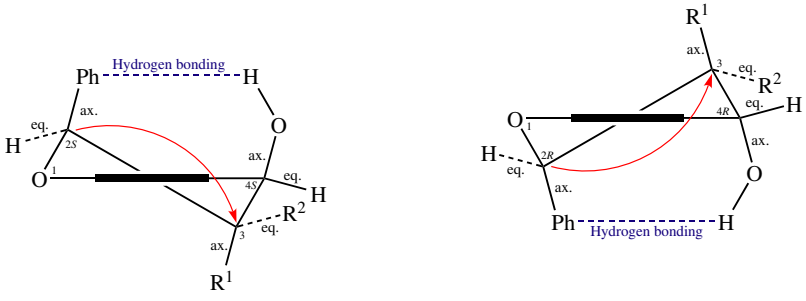


**A-conformer**

*P*-helicity ⇒ negative $^1L_b$ band

$R^1$ = H, $R^2$ = OH: (2*S*,3*S*,4*S*)-2,3-*cis*-3,4-*cis*

$R^1$ = OH, $R^2$ = H: (2*S*,3*R*,4*S*)-2,3-*trans*-3,4-*trans*

**A-conformer**

*M*-helicity ⇒ positive $^1L_b$ band

$R^1$ = H, $R^2$ = OH: (2*R*,3*R*,4*R*)-2,3-*cis*-3,4-*cis*

$R^1$ = OH, $R^2$ = H: (2*R*,3*S*,4*R*)-2,3-*trans*-3,4-*trans*

Fig. 22. A-conformation 2,4-*cis*-diaxial hydrogen bonding.

### 7.2. The $^1L_a$ transition

Ferreira et al. (2004) reported that the sign of the $^1L_a$ CE (ca. 240 nm) is the same as that for the $^1L_b$ CE (ca. 280 nm) for the all-*trans*-, all-*cis*- and 2,3-*cis*-3,4-*trans*-flavan-3,4-diols, except for the tetraacetate derivative of (+)-mopanol A. The sign of the $^1L_a$ CE (ca. 240 nm) seems to be opposite to the $^1L_b$ CE (ca. 280 nm) for the 2,3-*trans*-3,4-*cis*-flavan-3,4-diols, except for 2,3-*trans*,3,4-*cis*-leucocyanidin. It was also concluded that the CEs of the compounds under investigation did not consistently obey the DeAngelis–Wildman aromatic quadrant rule for correlating the $^1L_a$ CE sign with the absolute C4 configuration (DeAngelis and Wildman, 1969).

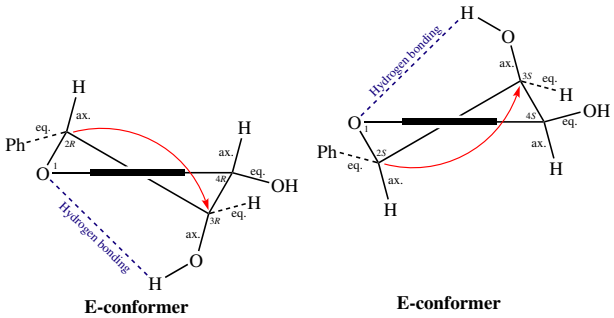


Fig. 23. E-conformation all-*cis* hydrogen bonding.

## 8. Flavans

Only a few flavans (**27**) have been reported to occur naturally, probably due to the fact that they are not readily visible on chromatograms and they have simple spectroscopic features compared to most other flavonoid classes (Bohm, 1998).

Flavans arise from a double reduction of a flavanone. Many flavans co-occur with the flavanone of identical substitution pattern. ORD and CD studies have revealed that all natural flavans have the 2*S* absolute configuration, as would be expected from the flavanone origin. Many of the natural flavans are listed as racemic due to a rotation of zero at 589 nm. The low specific rotation of flavans makes this a precarious assumption and their configuration can only be elucidated by studying their full CD data (Porter, 1988).

Antus et al. (2001) established that flavans have a half-chair conformation with the C2-phenyl group equatorial and that they follow the by now familiar rule of *P*-/*M*-helicity of the *O*-heterocyclic ring in the chroman

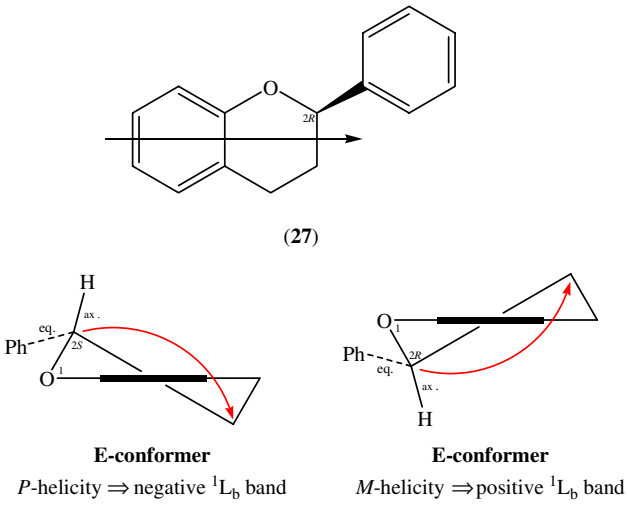


Fig. 24. Flavan (**27**) *P*- and *M*-helicity.

Table 10
Flavan CEs

| CE at $^1L_b$ (ca. 280 nm) | Helicity | Absolute configuration |
|---|---|---|
| Positive | *M* | (2*R*) |
| Negative | *P* | (2*S*) |

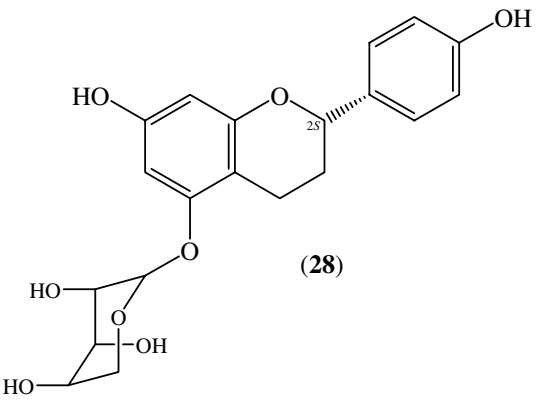


Fig. 25. (2*S*)-5,7,4′-trihydroxyflavan 5-*O*-β-D-xyloside (**28**).

chromophore leading to negative/positive CEs within the $^1L_b$ band. This implies that a negative $^1L_b$ CE is the result of 2*S* absolute configuration and a positive $^1L_b$ band the result of 2*R* absolute configuration (Fig. 24; Table 10).

The flavan glycoside (**28**), isolated from *Buckleya lanceolata* Miq. leaves, was reported by Sashida et al. (1976) and its absolute 2*S* configuration determined by CD spectroscopy (Fig. 25).

## 9. Isoflavans

Equol (7,4′-dihydroxyisoflavan), whose configuration was established as 3*S* (Kurosawa et al., 1968), is possibly the only flavonoid that was first obtained as an animal metabolite (Wong, 1975). Isoflavans (**29**) from plant origin always have an oxygen at C2′ and they almost never have oxygenation at C5 (Bohm, 1998).

Optical rotation measurements alone are not sufficient to assign absolute configuration to isoflavans. (3*S*)-isoflavans exhibit a negative CE in the 260–300 nm region of their ORD curves, but ORD and NMR measurements are markedly influenced by the preferred conformation of the molecule in solution (Kurosawa et al., 1978).

The favored conformation of the *O*-heterocyclic ring of isoflavans is expected to be the half-chair form, as for most other flavonoids and by analogy with cyclohexene and based on the minimization of torsional strain (Fig. 26). It is, however, not possible to state if the E- or A-conformer is of lower free energy, since the axial C3-phenyl (A-conformer) does not result in the familiar

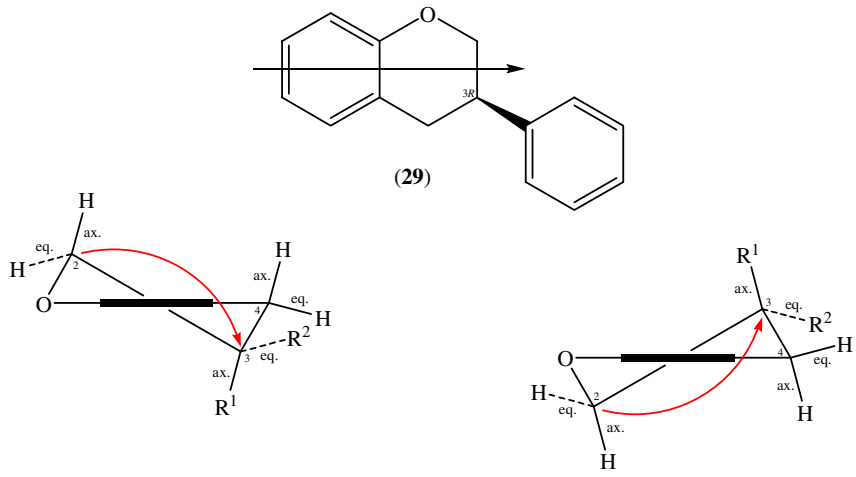


*P*-helicity ⇒ positive $^1L_b$ band / negative $^1L_a$ band
$R^1$ = H, $R^2$ = Ph: 3*R* - E-conformer
$R^1$ = Ph, $R^2$ = H: 3*S* - A-conformer

*M*-helicity ⇒ negative $^1L_b$ band / positive $^1L_a$ band
$R^1$ = H, $R^2$ = Ph: 3*S* - E-conformer
$R^1$ = Ph, $R^2$ = H: 3*R* - A-conformer

Fig. 26. Half-chair conformations for isoflavans (**29**).

destabilizing 1,3-diaxial interactions of axially substituted cyclohexane and cyclohexene systems (Eliel et al., 1965). The vicinal coupling constants ($J_{2,3}$ and $J_{3,4}$) for the isoflavans are, however, consistent with the values expected from the half-chair conformation (Emsley et al., 1968) with the C3-phenyl group equatorial (Kurosawa et al., 1968).

When using chiroptical methods for the establishment of absolute configuration of isoflavonoids, care should be taken to avoid problems caused by solvational effects upon the observed optical activity. The effects can be explained in terms of solvational and/or conformational equilibrium changes (Verbit and Clark-Lewis, 1968) and the problem can be alleviated by using the same solvent system for all the compounds under investigation.

Plain ORD curves above ca. 325 nm have been used to identify the absolute configuration of isoflavans (Suginome, 1966), but this has led to incorrect assignment of C3 configuration. ORD curves in the region of electronic absorption, however, gives a different picture (Verbit and Clark-Lewis, 1968), because the sign of the CE is a more accurate indicator of absolute configuration than the sign of the plain dispersion curve (Crabbé, 1965).

A study of the available ORD and CD data of isoflavans (Kurosawa et al., 1968, 1978; Verbit and Clark-Lewis, 1968; Donnelly et al., 1973; Woodward, 1980; Yahara et al., 1985; Clark-Lewis, 1962; Quaglia et al., 1991; Clark-Lewis et al., 1965; Hamburger et al., 1988; Versteeg et al., 1999) revealed that they follow an inverse helicity rule for the chroman chromophore compared to the flavonoids discussed thus far. This means that *P*-/*M*-helicity of the *O*-heterocyclic ring results in positive/negative CEs in the $^1L_b$ transition region (260–320 nm) and negative/positive CEs in the $^1L_a$ transition region (220–260 nm) (Fig. 26 and Table 11).

Table 11
Isoflavan CEs

| CE at $^1L_b$ (ca. 260–320 nm) | CE at $^1L_a$ (ca. 220–260 nm) | Helicity | Absolute configuration |
|---|---|---|---|
| Positive | Negative | *P* | (3*R*) |
| Negative | Positive | *M* | (3*S*) |

Although this rule is helpful in assigning absolute configuration to isoflavans, 2′,6′-disubstitution of the B-ring leads to different conformations of the *O*-heterocyclic ring due to steric effects (Fig. 27) and therefore to atypical ORD and CD curves (Wong, 1975). The NMR spectra of these compounds also reflect this conformational effect (Pelter and Amenechi, 1969).

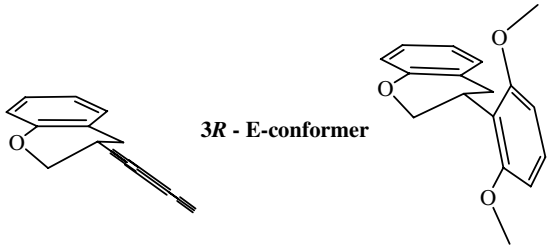


*P*-helicity ⇒ negative $^1L_a$ band *P*-helicity ⇒ positive $^1L_a$ band

Fig. 27. Conformation of 2′,6′-disubstituted isoflavans.

Versteeg et al. (1999) synthesized six isoflavans and their enantiomers (**31a/b-36a/b**), and used authentic 3*S*- and 3*R*-vestitol (**30a** and **30b**) derivatives to establish the absolute configuration at C3 of the synthetic isoflavans (Fig. 28). (3*S*)-isoflavans with oxygenation at both the A- and B-rings (**34a**, **35a** and **36a**) display positive and negative CEs in the 240 ($^1L_a$) and 270–280 nm ($^1L_b$) regions, respectively, and conversely for the 3*R*-enantiomers (**34b**, **35b** and **36b**) (Fig. 29). The

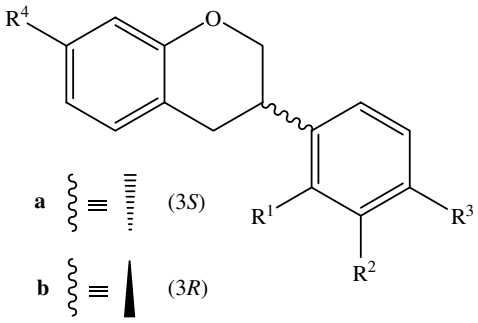


| Compound | $R^1$ | $R^2$ | $R^3$ | $R^4$ |
|---|---|---|---|---|
| **30a/b** | OH | H | OMe | OH |
| **31a/b** | H | H | OMe | H |
| **32a/b** | H | OMe | OMe | H |
| **33a/b** | OMe | H | OMe | H |
| **34a/b** | H | H | OMe | OMe |
| **35a/b** | OMe | H | H | OMe |
| **36a/b** | OMe | H | OMe | OMe |

Fig. 28. Synthetic isoflavans (**31a/b**–**36a/b**).

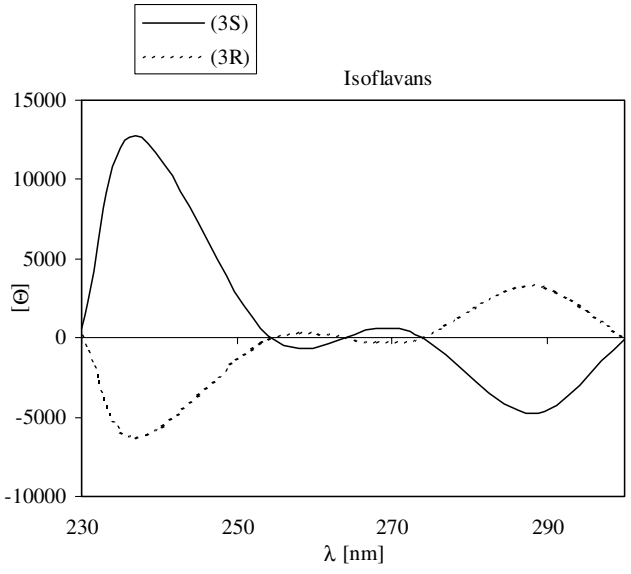


Fig. 29. CD spectra of isoflavans with oxygenation at both the A- and B-rings.

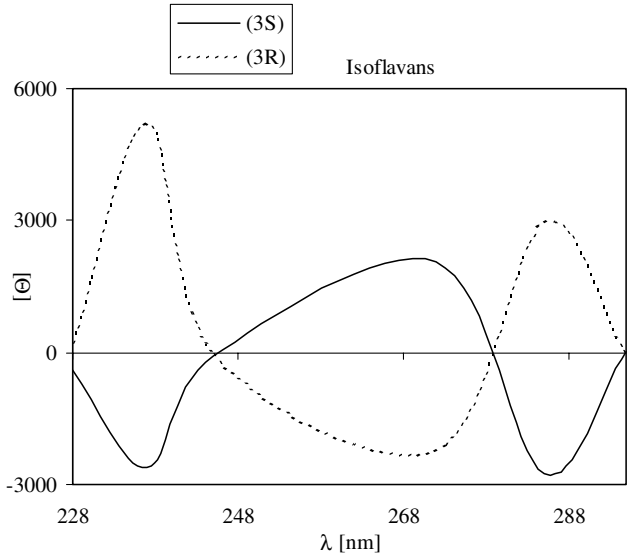


Fig. 30. CD spectra of 7-deoxy isoflavans with mono- and di-oxygenation on the B-ring.

7-deoxy 3*S*-isoflavans with mono- (**31a**) and di-oxygenation (**32a** and **33a**) on the B-ring displayed negative CEs in both the 230–240 ($^1L_a$) and 270–290 nm ($^1L_b$) regions, and conversely for the 3*R*-enantiomers (**31b**, **32b** and **33b**) (Fig. 30).

## 10. Isoflavanones

(3*R*)-Sophorol (2′,7-dihydroxy-4′,5′-methylenedioxyisoflavanone) was for many years the only natural optically active isoflavanone (**37**) known. Since racemization may occur under mild conditions, it was assumed that extraction and purification techniques were responsible for the observed isolation of optically inactive forms (Dewick, 1982). They show absorption at 200–240 and 260–300 nm ($\pi \rightarrow \pi^*$) and 320–352 nm ($n \rightarrow \pi^*$). A disproportionate number of the natural isoflavanones possess oxygenation at C2′ (Wong, 1975).

CD data is essential to assign absolute configuration to isoflavanones (Dewick, 1994). The octant rule modified for the cyclic arylketones (Snatzke, 1965a) predicts a positive CE for the $n \rightarrow \pi^*$ carbonyl transition for (3*R*)-isoflavanones with the B-ring in the favored equatorial position (Fig. 31). The equatorial orientation of the B-ring can be verified by NMR spectroscopic analysis with the coupling constant between the *trans*-diaxial $H2_\beta$ and H3 of ca. 11 Hz (Galeffi et al., 1997). Although assignments have been made using other absorption regions (Russell, 1997; Yahara et al., 1989), e.g., $^1L_a$, $^1L_b$ and $\pi \rightarrow \pi^*$, they seem to contradict each other and it is advisable to only use the $n \rightarrow \pi^*$ carbonyl transition for assignments (Table 12).

Galeffi et al. (1997) used CD to establish the absolute configuration of two prenylated isoflavanones (**38** and

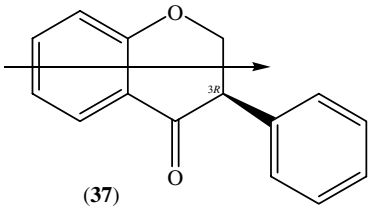


(**37**)

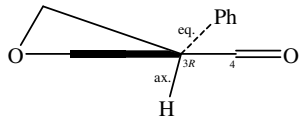


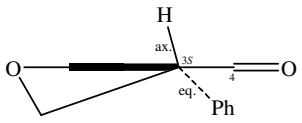


**E-conformer**

$3R \Rightarrow$ negative $^1L_a$ and positive n→ π* band

**E-conformer**

$3S \Rightarrow$ positive $^1L_a$ and negative n→ π* band

Fig. 31. Sofa conformations for isoflavanones (**37**).

Table 12
Isoflavanone CEs

| Absolute configuration | CE at n → π* (ca. 320–352 nm) |
|---|---|
| (3*R*) | Positive |
| (3*S*) | Negative |

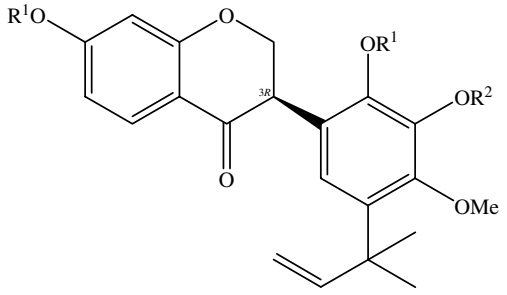


$R^1$ = H, $R^2$ = Me: Pervilleanone (**38**)
$R^1$ = Me, $R^2$ = Me: Dimethyl pervilleanone (**39**)

Fig. 32. Pervilleanone (**38**) and dimethyl pervilleanone (**39**).

**39**) as 3*R* using the n → π* carbonyl absorption band (Fig. 32).

## 11. Pterocarpans

Pterocarpans (**40**), 6a-hydroxypterocarpans (**41**) (Fig. 33), rotenoids (**42**), and 12a-hydroxyrotenoids (**43**) (Fig. 34) are members of the tetracyclic isoflavonoid subgroup of flavonoids (Bohm, 1998).

### 11.1. Pterocarpans

Pterocarpans contain two chiral centers, but only the (6a*R*,11a*R*)-*cis* and (6a*S*,11a*S*)-*cis* configurations are found in nature (Dewick, 1982, 1994; Szarvas et al., 2000). The *trans*-fused B/C-ring system (**45**) has been synthesized in racemic form (Van Aardt et al., 2001). It is accepted that all laevorotatory pterocarpans have the (6a*R*,11a*R*) absolute configuration, and dextrorotatory ones the (6a*S*,11a*S*) configuration (Wong, 1975; Dewick, 1982, 1988, 1994).

The preference in nature for the *cis* configuration over the *trans* has been established by computational

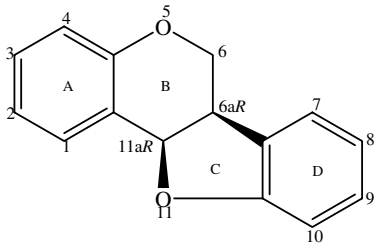


Pterocarpans (**40**)

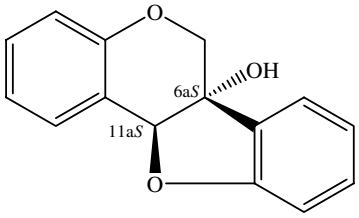


6a-Hydroxypterocarpans (**41**)

Fig. 33. Pterocarpans (**40**) and 6a-hydroxypterocarpans (**41**).

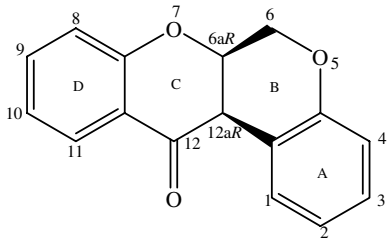


Rotenoids (**42**)

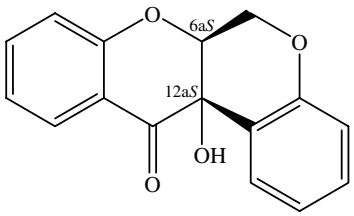


12a-Hydroxyrotenoids (**43**)

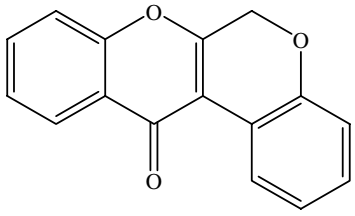


Dehydrorotenoids (**44**)

Fig. 34. Rotenoids (**42**), 12a-hydroxyrotenoids (**43**) and dehydrorotenoids (**44**).

studies that prove that a *trans*-fused B/C-ring system is energetically less favorable than the *cis*-fused system (Schöning and Friedrichsen, 1989). Although two strain-free conformations can exist, the preferred one is that in which the pyran B-ring approximates to a half-chair with the D-ring quasi-equatorial, making H6$_\beta$ quasi-axial and H6$_\alpha$ quasi-equatorial (Fig. 35; Friedrichsen and Schöning, 1990). In other words, the preferred conformation is a 6a,11a-di-pseudo-axially substituted arrangement with the B-ring in a half-chair form, giving a truly staggered conformation along the C6–C6a axis. This served as confirmation of what had earlier been found through the study of $^1$H NMR coupling constants (Pachler and Underwood, 1967).

The UV spectra of simple pterocarpans generally display a major peak at ca. 285–310 nm and a smaller band at ca. 280–287 nm, while their ORD spectra show multiple CEs in the 250–350 nm region, which may also be used to assign absolute configuration (Cook et al., 1978).

The chroman (A- plus B-ring) and 2,3-dihydrobenzo[b]furan (C- plus D-ring) chirally perturbed achiral chromophores are concurrently present in the *cis* annulated pterocarpans. The CD bands of these compounds

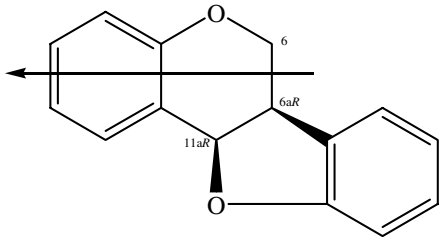


(**40**)

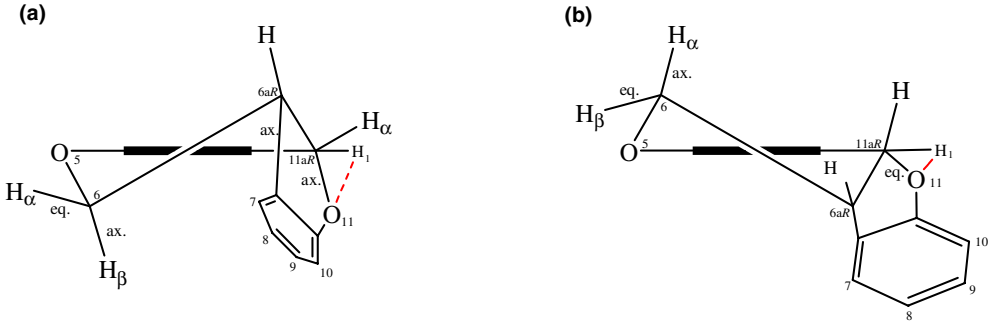


Fig. 35. (−)-(6a*R*,11a*R*)-*cis*-pterocarpans (**40**). The dashed (red) line indicates steric interaction between pseudo-axially O11 and *peri*-standing H1. (a) Lower and (b) higher energy conformation.

are assigned as follows: $^1L_a$ at ca. 220–240 nm, $^1L_b$ at ca. 260–310 nm, and $^1B_b$ at ca. 200 nm. Positive/negative $^1L_b/^1L_a$ CEs of the major bands indicates (6a*R*,11a*R*) configuration, and vice versa for (6a*S*,11a*S*). The $^1L_b$ band may split or have a shoulder with smaller intensity at shorter wavelength, which may be attributed to the $^1L_b$ band contribution of the 2,3-dihydrobenzo[*b*]furan chromophore. The exciton coupled interaction between the $^1L_b$ bands of the chirally perturbed chroman and 2,3-dihydrobenzo[*b*]furan chromophores can, however, be excluded (Antus et al., 2001).

The chroman ring is the dominant chromophore in the pterocarpans as indicated by the high intensity of the $^1L_b$ band. The sign of the low energy/high wavelength $^1L_b$ band reflects the helicity of the second-sphere (B-ring), while the high energy/low wavelength $^1L_a$ band possibly reflects the contribution of the third-sphere (C- and D-ring). The benzylic C-ring oxygen (O11) is pseudo-axially oriented (Fig. 35) to avoid steric interaction with the *peri*-hydrogen at C1. A substituent in a pseudo-axial position at the benzylic atom gives rise to sign inversion in both the $^1L_a$ and $^1L_b$ CD bands of the chroman chromophore. Therefore, the positive $^1L_b$ band and the negative $^1L_a$ band correlate with *P*-helicity of the B-ring in all naturally occurring (−)-(6a*R*,11a*R*)-*cis*-pterocarpans (Fig. 36). The CD features of pterocarpans are determined by these bands and can be used unequivocally for their absolute configurational assignment, since different substitution patterns of the aromatic A-ring do not alter the sign of the $^1L_b$ band of the chiral chroman chromophore (Antus et al., 2001).

Thus, due to the pseudo-axial substituents at benzylic position (C11a in the chroman and C6a in the 2,3-dihydrobenzo[b]furan moiety), both chromophores show

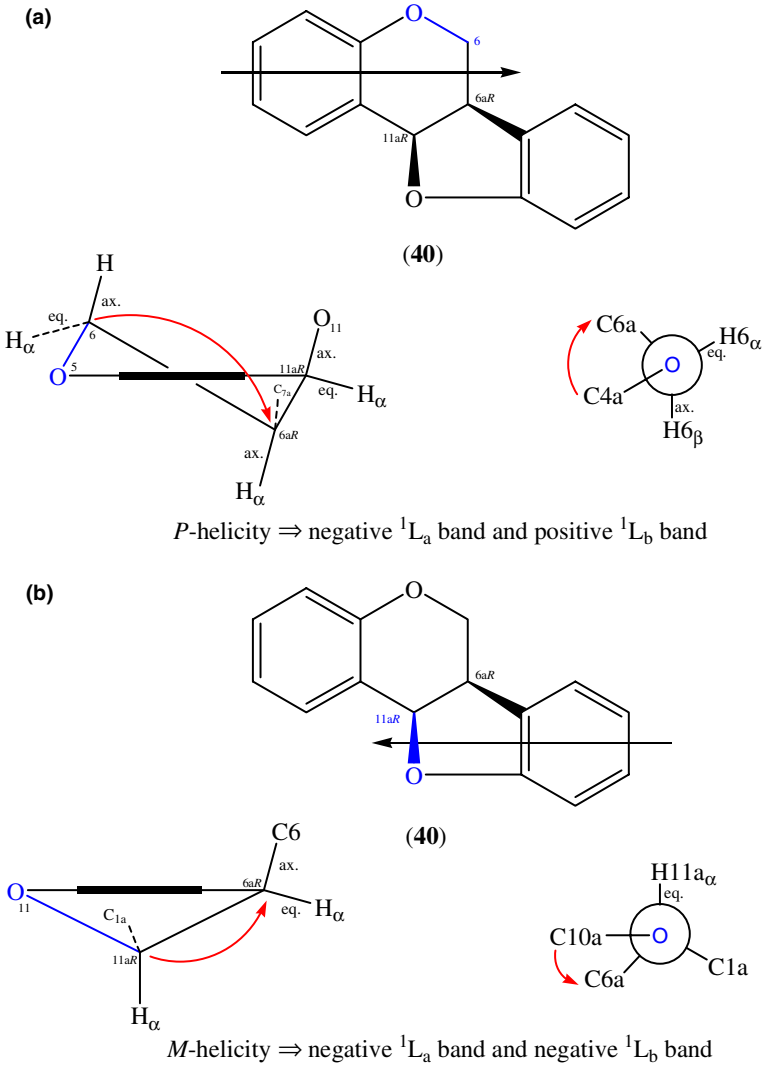


Fig. 36. Helicity of (−)-(6a*R*,11a*R*)-*cis*-pterocarpans (**40**). (a) *P*-Helicity (indicated by the red arrow) of the chroman chromophore. Newman projection viewing along the O5–C6 axis (indicated in blue). (b) *M*-helicity (indicated by the red arrow) of the 2,3-dihydrobenzo[*b*]furan chromophore. Newman projection viewing along the O11–C11a axis (indicated in blue).

anomalous behavior in *cis*-pterocarpans. The helicity rules for *cis*-pterocarpans are therefore opposite to those observed for isolated chroman (Antus et al., 1994) and 2,3-dihydrobenzo[*b*]furan (Kurtán et al., 2000) chromophores bearing no axial benzylic substituents (Table 13; Kiss et al., 2003).

The $^1$H NMR coupling constants between H6a and H11a (ca. 13.4 Hz) prove the *trans* diaxial orientation of these protons and the equatorial orientation of O11 and C7a (Van Aardt et al., 2001) in (6a*S*,11a*R*)-*trans*-pterocarpans (**45**). Consequently, there are no axial substituents to influence resolutely the CD properties of the

Table 13
*cis*-Pterocarpan CEs

| Chroman chromophore | | 2,3-Dihydrobenzo[*b*]furan chromophore | | CE at $^1L_a$ (ca. 220–250 nm) | $[\alpha]_D$ | Absolute configuration |
|---|---|---|---|---|---|---|
| CE at $^1L_b$ (ca. 260–310 nm) | Helicity | CE at $^1L_b$ (ca. 260–310 nm) | Helicity | | | |
| Positive | *P* | Negative | *M* | Negative | – | (6a*R*,11a*R*) |
| Negative | *M* | Positive | *P* | Positive | + | (6a*S*,11a*S*) |

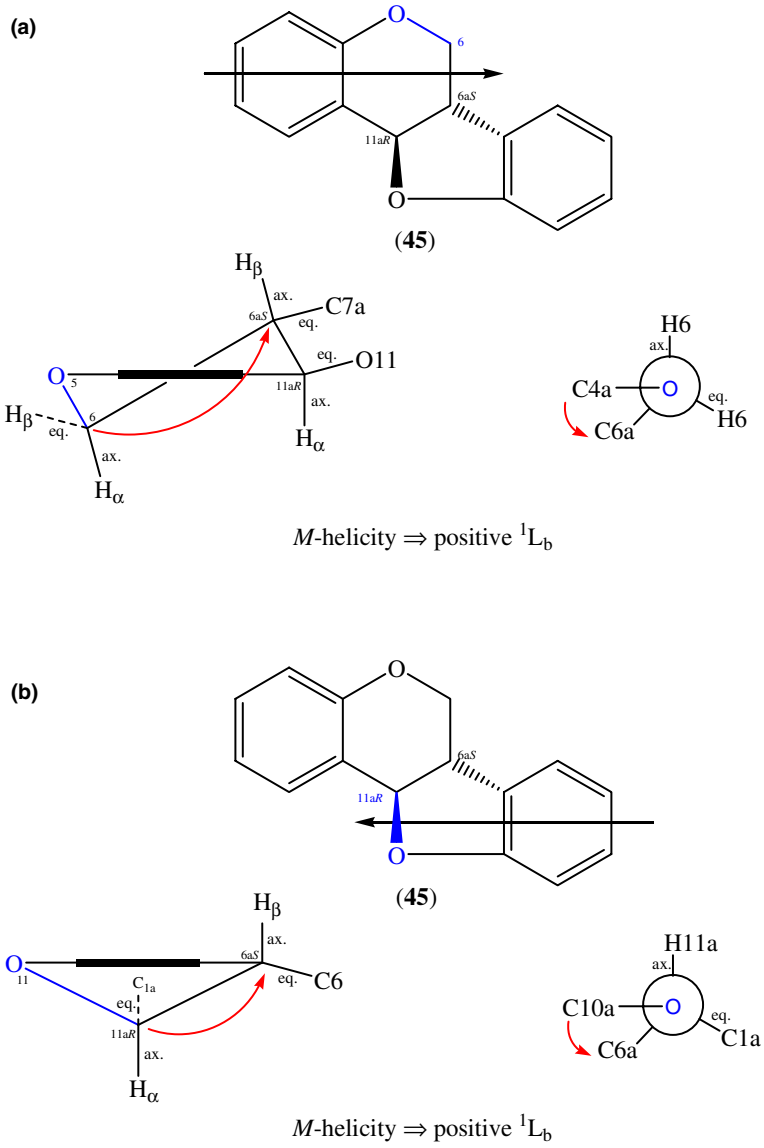


Fig. 37. Helicity of (−)-(6a*S*,11a*R*)-*trans*-pterocarpans (**45**). (a) *M*-helicity (indicated by the red arrow) of the chroman chromophore. Newman projection viewing along the O5–C6 axis (indicated in blue). (b) *M*-helicity (indicated by the red arrow) of the 2,3-dihydrobenzo[*b*]furan chromophore. Newman projection viewing along the O11–C11a axis (indicated in blue).

Table 14
*trans*-Pterocarpan CEs

| Chroman chromophore | | 2,3-Dihydrobenzo[b]furan chromophore | | $[\alpha]_D$ | Absolute configuration |
|---|---|---|---|---|---|
| CE at $^1L_b$ (ca. 260–310 nm) | Helicity | CE at $^1L_b$ (ca. 260–310 nm) | Helicity | | |
| Positive | M | Positive | *M* | + | (6a*S*,11a*R*) |
| Negative | *P* | Negative | *P* | – | (6a*R*,11a*S*) |

unnatural (6a*S*,11a*R*)-*trans*-pterocarpans (Fig. 37). Therefore, the original helicity rules of the isolated chromophores are valid: positive $^1L_b$ band corresponds to *M*-helicity in both the five- and six-membered *O*-hetero-ring chromophores, namely, the C- and B-ring, respectively.

In summary, the chiral second spheres, namely, the helicities of the *O*-heterocyclic rings, determine the sign of the characteristic CD bands of (6a*S*,11a*R*)-*trans*-pterocarpans. This implies that *M*-helicity of both the chroman and the 2,3-dihydrobenzo[b]furan chromophore leads to a positive $^1L_b$ band (Table 14; Kiss et al., 2003).

### 11.2. 6a-Hydroxypterocarpans

As with *cis*-pterocarpans, the optical activity of *cis*-6a-hydroxypterocarpans can be correlated with absolute configuration. Laevorotatory compounds, thus, have the (6a*S*,11a*S*)-*cis* configuration and dextrorotatory compounds the (6a*R*,11a*R*)-*cis* configuration (Table 15; Figs. 38 and 39; Dewick, 1994).

Table 15
6a-Hydroxypterocarpan CEs

| CE at $^1L_b$ (ca. 270–300 nm) | CE at $^1L_a$ (ca. 220–250 nm) | Helicity | $[\alpha]_D$ | Absolute configuration |
|---|---|---|---|---|
| Negative | Positive | *P* | + | (6a*R*,11a*R*)-*cis* |
| Positive | Negative | *M* | – | (6a*S*,11a*S*)-*cis* |
| Negative | Negative | *M* | + | (6a*S*,11a*R*)-*trans* |
| Positive | Positive | *P* | – | (6a*R*,11a*S*)-*trans* |

For *trans*-6a-hydroxypterocarpans (**45** and **46**), however, an inversion of configuration compared to pterocarpans occurs: laevorotatory compounds have (6a*R*,11a*S*)-*trans* configuration (**46**) and dextrorotatory

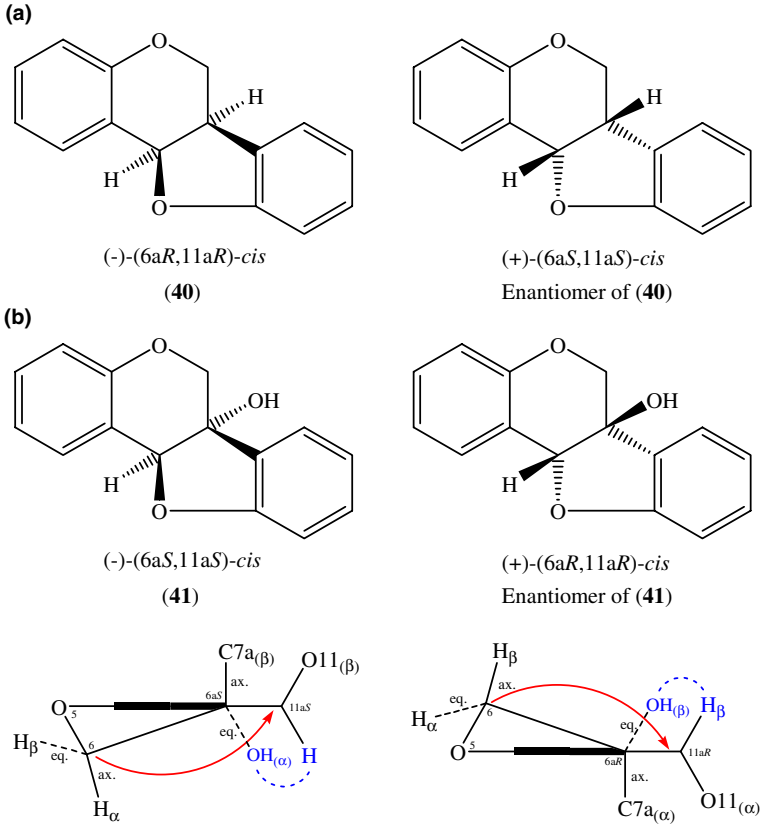


Fig. 38. (a) *cis*-Pterocarpans [(**40**) and enantiomer of (**40**)] and (b) *cis*-6a-hydroxypterocarpans [(**41**) and enantiomer of (**41**)].

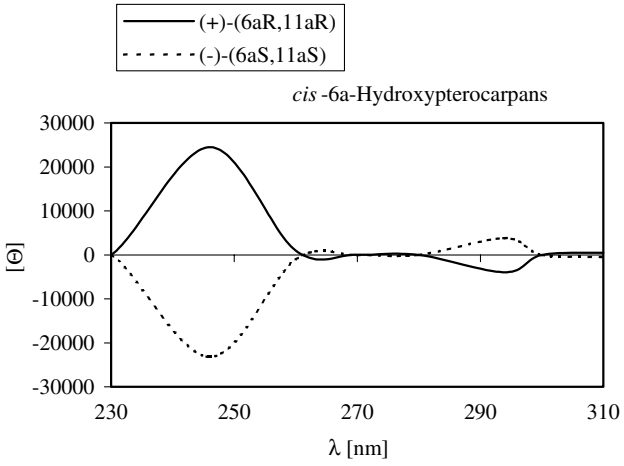


Fig. 39. CD spectra of *cis*-6a-hydroxypterocarpans.

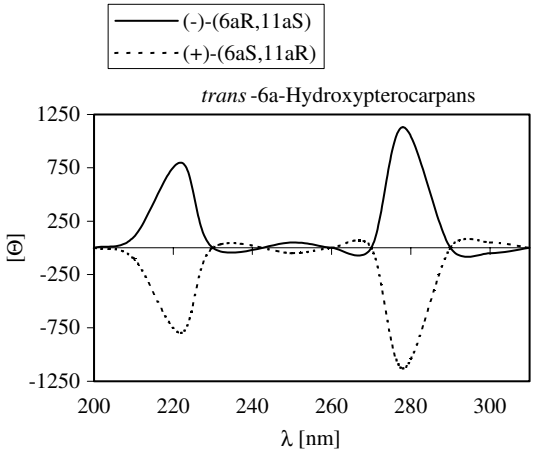


Fig. 41. CD spectra of *trans*-6a-hydroxypterocarpans.

compounds (6a*S*,11a*R*)-*trans* configuration (**45**) (Table 15; Figs. 40 and 41; Van Aardt et al., 2001).

The protons of the hetero-ring of *cis*- and *trans*-6a-hydroxypterocarpans resonate in the $^{1}$H NMR spectra as a geminal AB-system and as broadened singlets for C6a–OH. Shielding of H11a in the *trans*-isomer relative to the *cis*-isomer results from the fact that H11a is axially oriented relative to the aromatic A- and D-rings

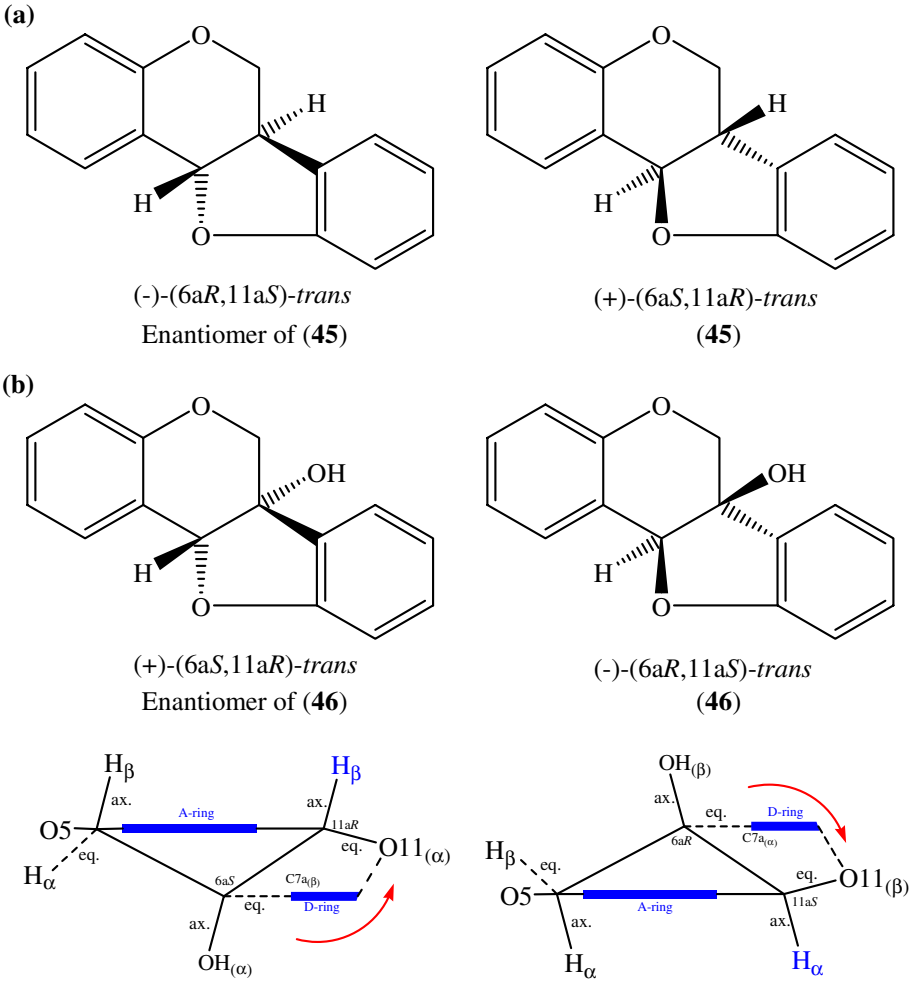


Fig. 40. (a) *trans*-Pterocarpans [(**45**) and enantiomer of (**45**)] and (b) *trans*-6a-hydroxypterocarpans [(**46**) and enantiomer of (**46**)].

Table 16
Rotenoid CEs

| NMR: δH1 | B/C-ring fusion | $[\alpha]_D$ | CE at π–π* (ca. 300–330 nm) | CE at $n \rightarrow \pi^*$ (ca. 348–360 nm) | Absolute configuration |
|---|---|---|---|---|---|
| 6.6–6.8 | *cis* | + | Positive | Negative | (6a*R*,12a*R*) |
| | | – | Negative | Positive | (6a*S*,12a*S*) |
| 7.6–7.9 | *trans* | + | Negative | Positive | (6a*S*,12a*R*) |
| | | – | Positive | Negative | (6a*R*,12a*S*) |

Table 17
12a-Hydroxyrotenoid CEs

| NMR: δH1 | B/C-ring fusion | $[\alpha]_D$ | CE at π–π*(ca. 300–330 nm) | CE at n → π* (ca. 348–360 nm) | Absolute configuration |
|---|---|---|---|---|---|
| 6.6–6.8 | *cis* | + | Positive | Negative | (6a*S*,12a*S*) |
| | | – | Negative | Positive | (6a*R*,12a*R*) |
| 7.6–7.9 | *trans* | + | Negative | Positive | (6a*R*,12a*S*) |
| | | – | Positive | Negative | (6a*S*,12a*R*) |

in the former isomer (Fig. 40). NOESY interactions between C6a–OH and H11a in the *cis*-isomer (Fig. 38) are absent in the *trans*-isomer (Fig. 40), indicating the *trans*-B/C-ring geometry (Van Aardt et al., 2001).

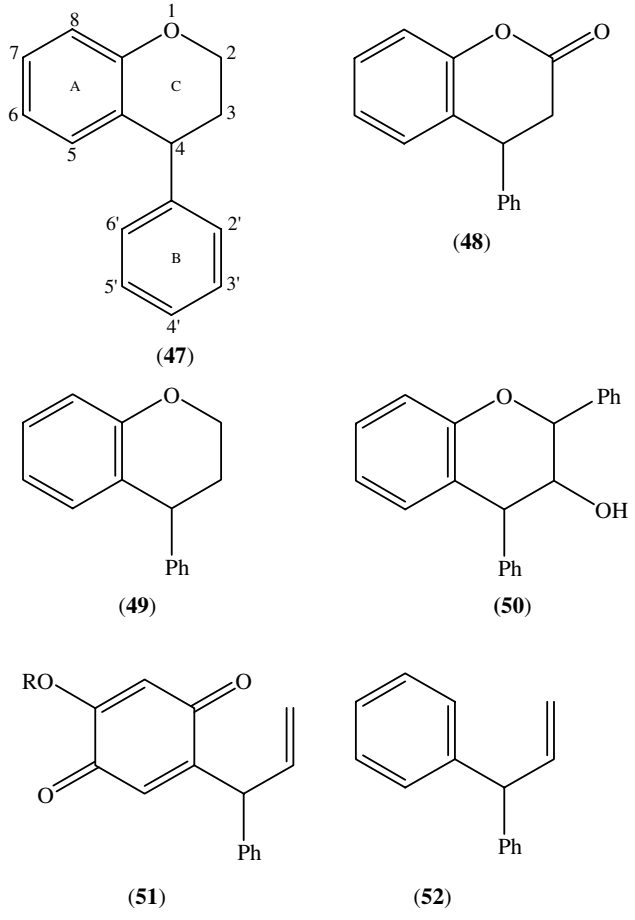


Fig. 42. C6.C3.C6 4-arylchroman skeleton (**47**), 3,4-dihydro-4-arylcoumarins (**48**), 4-arylchromans (**49**), 4-arylflavan-3-ols (**50**), dalbergiones (**51**), and dalbergiquinols (**52**).

## 12. Rotenoids

Rotenoids are a class of isoflavonoids that arises in nature by oxidative cyclization of a 2′-methoxyisoflavone. They are characterized by the inclusion of an extra carbon atom (C12) into an additional heterocyclic ring (ring C) and are subdivided into three major types according to oxidation levels in the rotenoid ring system, namely rotenoids (**42**), 12a-hydroxyrotenoids

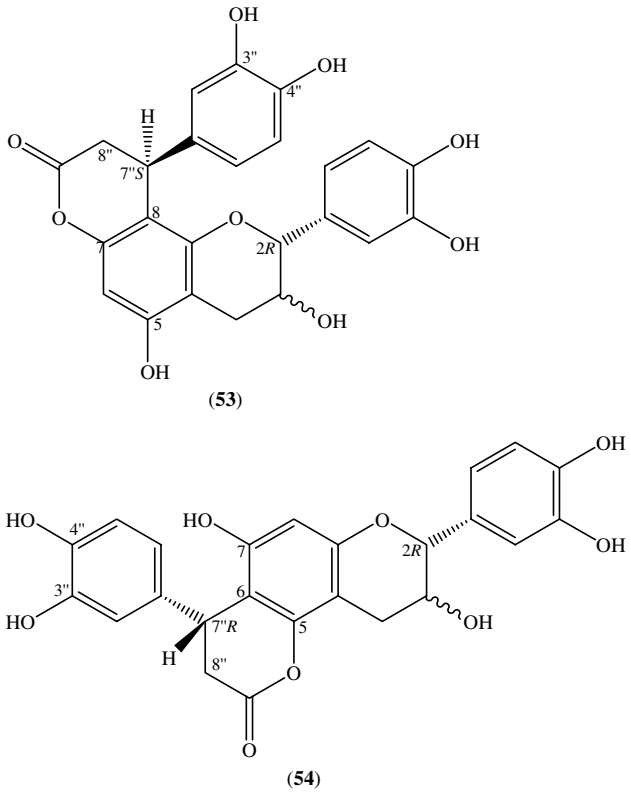


Fig. 43. Phenylpropanoid-substituted flavan-3-ols. 5,7,8-Trisubstituted compounds (**53**) and 5,6,7-trisubstituted compounds (**54**).

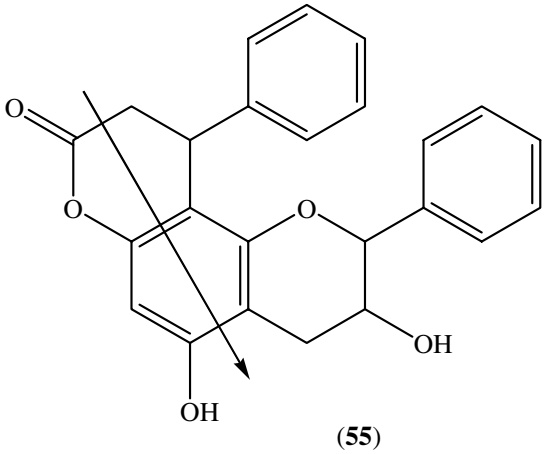


(**55**)

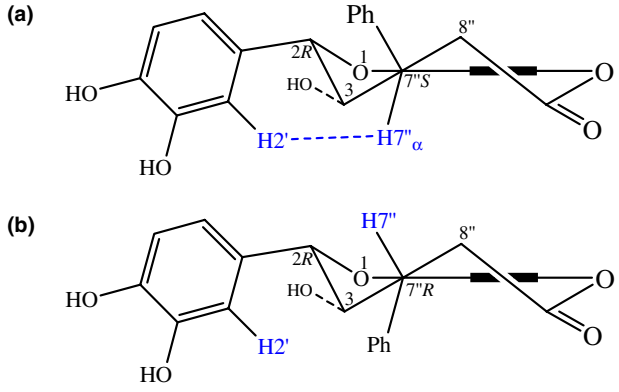


Fig. 44. NOESY interaction (blue dashed line) between H7″ and H2′ in neoflavonoids (**55**). (a) (7″*S*)-neoflavonoid and (b) (7″*R*)-neoflavonoid.

(rotenolones) (**43**) and dehydrorotenoids (**44**) (Fig. 34; Dewick, 1994).

The absolute configurations of almost all of the known natural rotenoids are the same as those found in (−)-rotenone, i.e., *cis*-(6a*S*,12a*S*) (Dewick, 1994; Djerassi et al., 1961; Büchi et al., 1961). The root bark of *Piscidia erythrina* yielded the first known rotenoid possessing a *cis*-(6a*R*,12a*R*) absolute configuration, namely (+)-erythynone (Tahara et al., 1990).

Natural rotenoids have the thermodynamically favored *cis*-fused B/C-ring system, indicated by the

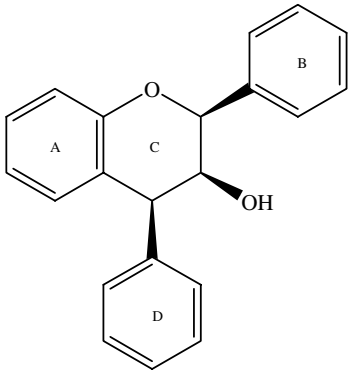


(2*S*,3*S*,4*S*)
(**56**)

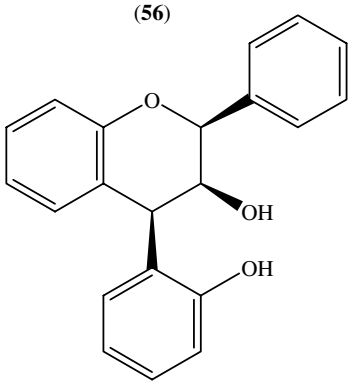


(2*S*,3*S*,4*S*)
(**57**)

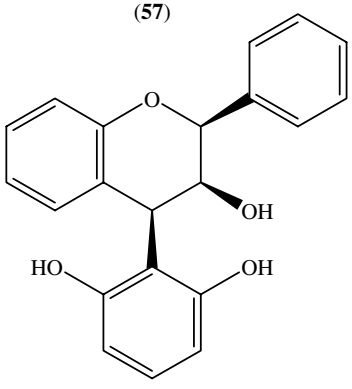


(2*S*,3*S*,4*R*)
(**58**)

Fig. 45. Cahn–Ingold–Prelog priorities for 4-arylflavan-3-ols (**56**–**58**).

Table 18
4-Arylflavan-3-ol CEs

| C2 | NMR: $J_{2,3}$ | NMR: $J_{3,4}$ | CE [220–240 nm] | Helicity | C4-aryl | Absolute configuration |
|---|---|---|---|---|---|---|
| *S* | *cis* | *cis* | Negative | *M* | Above | (2*S*,3*S*,4*S*) |
| | | *trans* | Negative | | Below | (2*S*,3*S*,4*R*) |
| | *trans* | *cis* | Negative | | Below | (2*S*,3*R*,4*R*) |
| | | *trans* | Positive | | Above | (2*S*,3*R*,4*S*) |
| *R* | *cis* | *cis* | Positive | *P* | Below | (2*R*,3*R*,4*R*) |
| | | *trans* | Positive | | Above | (2*R*,3*R*,4*S*) |
| | *trans* | *cis* | Positive | | Above | (2*R*,3*S*,4*S*) |
| | | *trans* | Negative | | Below | (2*R*,3*S*,4*R*) |

chemical shift of H1 at $\delta$ 6.6–6.8 in $CDCl_3$, acetone-$d_6$, acetonitrile-$d_3$ and benzene-$d_6$, at $\delta$ 6.4 in DMSO-$d_6$ and at $\delta$ 7.3 in pyridine-$d_5$ (Crombie and Lown, 1961, 1962; Carlson et al., 1973; Oberholzer et al., 1974). The B- and C-ring conformations implied by these coupling constants are appropriately described with dihedral angles of 65° and 55°, estimated from a Dreiding model (Kostova et al., 1991) and confirmed by X-ray studies, which confirmed the predominance of this conformer, as well as the bent nature of the molecule resulting from the *cis*-B/C-ring fusion (Begley et al., 1975).

Natural rotenoids without substituents at C12 have *cis*-fused B/C ring systems, but when a hydroxyl group is present at C12, both *cis* and *trans* geometry may occur (Yenesew et al., 2003).

The unnatural *trans*-fused system has been synthesized by 1,4-reduction of dehydrorotenoids with DIBAL yielding (±)-*trans*-isorotenone, the configuration of which was confirmed by X-ray crystallography (Begley et al., 1989). The *trans*-B/C series is characterized by the strongly deshielded H1 at $\delta$ 7.6-7.9 in $CDCl_3$, acetone-$d_6$ and methanol-$d_4$, and at $\delta$ 8.2–8.5 in pyridine-$d_5$ (Crombie and Lown, 1961, 1962; Unai et al., 1973). If the A-ring has no methoxy substituents, the chemical shift of H1 is moved down-field to $\delta$ 8.33 in $CDCl_3$ (Santos et al., 1998), 8.2 in DMSO-$d_6$ and 8.65 in acetone-$d_6$ (Shawl et al., 1988). There are two possible conformers with a *trans*-B/C ring junction as defined by the relative configuration of H6a to the two C6 protons, in which H6a can be equatorial or axial (Yenesew et al., 1998).

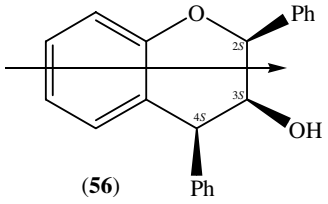


(**56**)

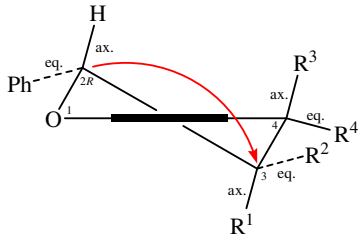


| C2/C3 | C3/C4 | C2 | C3 | C4 | $R^1$ | $R^2$ | $R^3$ | $R^4$ | Helicity |
|---|---|---|---|---|---|---|---|---|---|
| *cis* | *cis* | *R* | *R* | *R* | OH | H | H | Ph | *P* |
| *trans* | *trans* | *R* | *S* | *R* | H | OH | H | Ph | *P* |
| *cis* | *trans* | *R* | *R* | *S* | OH | H | Ph | H | *P* |
| *trans* | *cis* | *R* | *S* | *S* | H | OH | Ph | H | *P* |

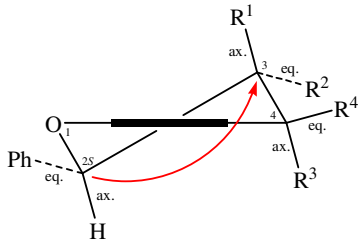


| C2/C3 | C3/C4 | C2 | C3 | C4 | $R^1$ | $R^2$ | $R^3$ | $R^4$ | Helicity |
|---|---|---|---|---|---|---|---|---|---|
| *cis* | *cis* | *S* | *S* | *S* | OH | H | H | Ph | *M* |
| *trans* | *trans* | *S* | *R* | *S* | H | OH | H | Ph | *M* |
| *cis* | *trans* | *S* | *S* | *R* | OH | H | Ph | H | *M* |
| *trans* | *cis* | *S* | *R* | *R* | H | OH | Ph | H | *M* |

Fig. 46. Half-chair conformation for 4-arylflavan-3-ols.

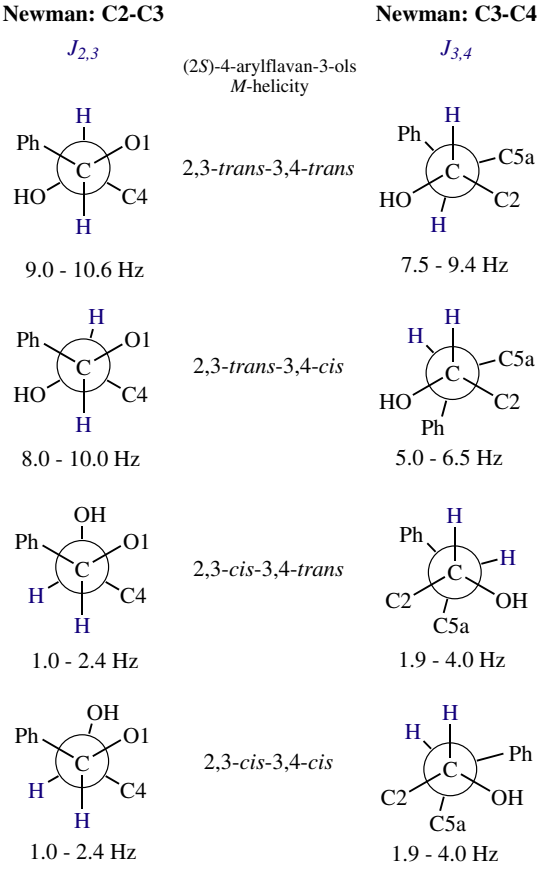


Fig. 47. Couplings constants ($J_{2,3}$ and $J_{3,4}$) for 4-arylflavan-3-ols. Newman projections for (2*S*)-4-arylflavan-3-ols (*M*-helicity).

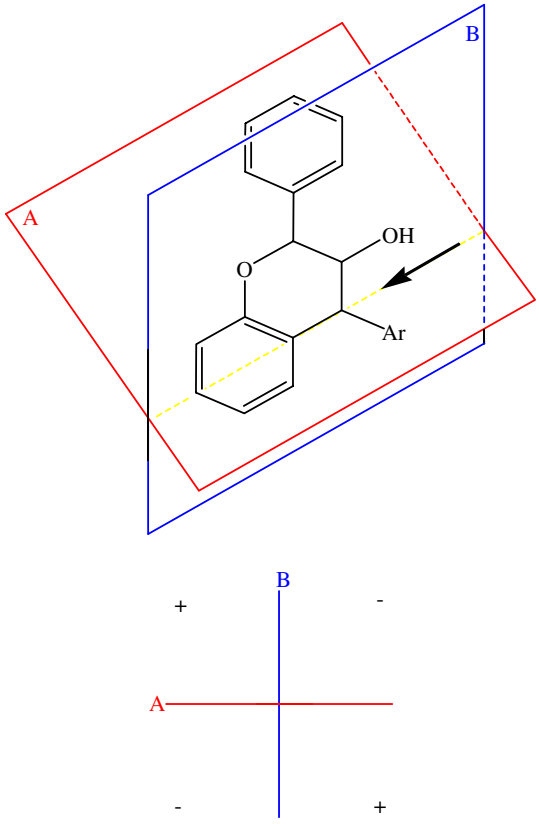


Fig. 49. Aromatic quadrant rule.

A 1,2-*trans*-diaxial relationship is identified by a large coupling constant ($J \sim 11$–$12$ Hz) between H6a and one of the C6 protons (Fukami and Nakajima, 1971).

Once the B/C-ring fusion is established as either *cis* or *trans* by $^1$H NMR spectroscopic analysis, CD data can be used to determine the absolute configurations at C6a and C12a (Ollis et al., 1967; Lami et al., 1990; Tahara et al., 1990; Yenesew et al., 1998). Due to the presence of several chromophores with relatively strong absorption in the 360–190 nm range, the CD spectra of rotenoids show multiple CEs. The longer wavelength CE around 350 nm arising from n → π* transition of the acetophenone chromophore and the CE around 320 nm, associated with longest wavelength aromatic π → π* transition of ring A, are used to establish absolute configuration (Tables 16 and 17; Kostova et al., 1991).

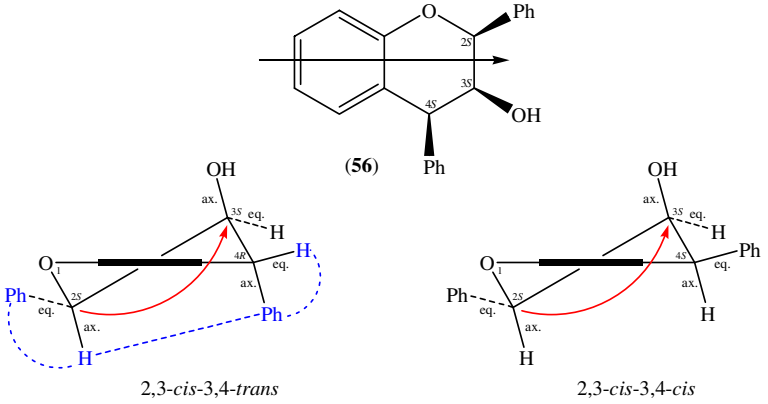


Fig. 48. NMR interactions for 2,3-*cis*-3,4-*trans*-isomers: secondary couplings of H2 and H4 with aromatic protons and interaction between H2-axial and C4-phenyl-quasi-axial (indicated in blue).

## 13. Neoflavonoids

The neoflavonoids are a group of $C_{15}$ naturally occurring compounds having a C6.C3.C6 4-arylchroman skeleton (**47**). They are closely related in structure and biogenetics to the flavonoids and isoflavonoids (Fig. 42, Donnelly and Boland, 1994).

The chiral analogues can be subdivided into the following groups: 3,4-dihydro-4-arylcoumarins (**48**), 4-arylchromans (**49**), 4-arylflavan-3-ols (**50**), and acyclic neoflavonoids like (**51**) and (**52**) (Fig. 42).

### *13.1. 3,4-Dihydro-4-arylcoumarins*

A series of phenylpropanoid-substituted flavan-3-ols, e.g., (**53**) and (**54**), have been isolated from different sources (Fig. 43; Nonaka and Nishioka, 1982; Foo, 1987, 1989; Chen et al., 1993; Fan et al., 1999). According to Chen et al. (1993), the absolute configuration of the C7″ methine carbon of the 5,7,8-trisubstituted compounds can be established by considering the NOESY interaction between H7″ and H2′ of the (2*R*)-flavan-3-ol unit, which is only present when the absolute configuration of C7″ is *S*, with H7″ in an α position (Fig. 44). CD can then be used to establish the absolute configuration of other similar compounds. Phenylpropanoid-substituted flavan-3-ols with 7″*S* configuration will display negative CEs at ca. 225–234 and 275-284 nm and a positive CE at 250–255 nm, and vice versa for 7″*R* compounds.

### *13.2. 4-Arylflavan-3-ols*

The first 4-arylflavan-3-ol was isolated from the dimeric fraction of the succulent, *Nelia meyeri* (Kolodziej, 1983, 1984).

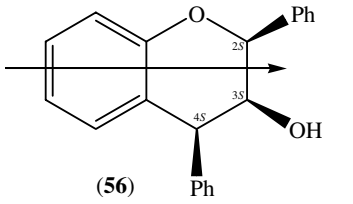


(**56**)

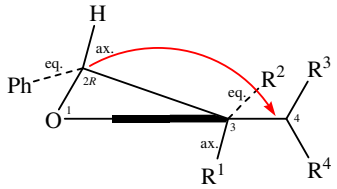


| C2/C3 | C3/C4 | C2 | C3 | C4 | $R^1$ | $R^2$ | $R^3$ | $R^4$ | Helicity |
|---|---|---|---|---|---|---|---|---|---|
| *cis* | *cis* | *R* | *R* | *R* | OH | H | H | Ph | *P* |
| *trans* | *trans* | *R* | *S* | *R* | H | OH | H | Ph | *P* |
| *cis* | *trans* | *R* | *R* | *S* | OH | H | Ph | H | *P* |
| *trans* | *cis* | *R* | *S* | *S* | H | OH | Ph | H | *P* |

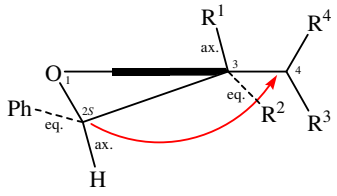


| C2/C3 | C3/C4 | C2 | C3 | C4 | $R^1$ | $R^2$ | $R^3$ | $R^4$ | Helicity |
|---|---|---|---|---|---|---|---|---|---|
| *cis* | *cis* | *S* | *S* | *S* | OH | H | H | Ph | *M* |
| *trans* | *trans* | *S* | *R* | *S* | H | OH | H | Ph | *M* |
| *cis* | *trans* | *S* | *S* | *R* | OH | H | Ph | H | *M* |
| *trans* | *cis* | *S* | *R* | *R* | H | OH | Ph | H | *M* |

Fig. 50. Sofa conformation for 4-arylflavan-3-ols.

Stereoselective condensation at C4 of flavan-3,4-diols of known absolute configuration with phloroglucinol and resorcinol proceeds at ambient temperatures with either partial or complete retention of configuration for the 2,3-*trans*-isomers and with inversion for 2,3-*cis* isomers (Botha et al., 1978). The CD spectra of the resultant 2,3-*trans*- and 2,3-*cis*-4-arylflavan-3-ols are dominated by multiple CEs contributed by the C4-aryl chromophore when compared to the CEs of flavan-3-ols.

The CD curves of the methyl ether 3-acetates of the synthesized 4-arylflavan-3-ols showed that CEs due to chirality at C2 and C3 are completely dominated by the multiple high amplitude CEs of the C4-aryl chromophore (220–240 nm). A positive CE indicates a quasi-axial (extending above the plane of the fused A-ring) C4-aryl group, and a negative CE indicates a quasi-equatorial (extending below the plane of the fused A-ring) C4-aryl group (Table 18).

Care has to be taken with assignment of *R* and *S* absolute configuration at C4, since substituents on the D-ring influences the CIP priorities (Figs. 45 and 46; Cahn et al., 1956, 1966).

The $^1$H NMR coupling constants of the heterocyclic protons of the methyl ether 3-acetates of the 4-arylflavan-3-ols vary considerably, but are, with exceptions, consistent with the relative configuration for 2,3-*trans*-3,4-*trans*- ($J_{2,3}$ 9.0–10.6, $J_{3,4}$ 7.5–9.4 Hz) and 2,3-*trans*-3,4-*cis*- ($J_{2,3}$ 8.0–10.0, $J_{3,4}$ 5.0–6.5 Hz) analogues (Fig. 47; Baig et al., 1969a,b; Clark-Lewis et al., 1964). The 2,3-*cis*-3,4-*trans*-isomers ($J_{2,3}$ 1.0–2.4, $J_{3,4}$ 1.9–4.0 Hz) are distinguished from their 2,3-*cis*-3,4-*cis*-counterparts by NOE experiments and by extensive secondary couplings of H2 and H4 with aromatic protons, and by strong interaction between the C2-axial proton and C4-quasi-axial phenyl groups (Fig. 48; Botha et al., 1981b).

CD data of methyl ether 3-acetates of 2,3-*cis*-3,4-*cis*-4-arylflavan-3-ols and the catechin-4α-phloroglucinol analogue with abnormal coupling constants ($J_{2,3}$ 6.5, $J_{3,4}$ 5.5 Hz) exhibit inverse CEs to the above mentioned rule (Table 18; Van der Westhuizen et al., 1981). This indicates that deviations from the normal dihedral angles between substituents on the heterocyclic ring, and therefore from the expected half-chair conformations, significantly influences the sign of the CE. The aromatic quadrant rule (Fig. 49; DeAngelis and Wildman, 1969) can be used to explain the observed inversion of CEs. Substituents in the upper left and lower right quadrants make positive contributions to the 220–240 nm band and substituents in the upper right and lower left quadrants make a negative contribution. The C4-aryl is attached directly to the chiral center and will therefore contribute the major part of the sign of the high-intensity low-wavelength CE.

Half-chair (Fig. 46) and sofa (Fig. 50) preferred conformations of the heterocyclic rings of 2,3-*trans*-3,4-*trans*-, 2,3-*trans*-3,4-*cis*-, and 2,3-*cis*-3,4-*trans*-4-arylflavan-3-ols results in a correct correlation between the

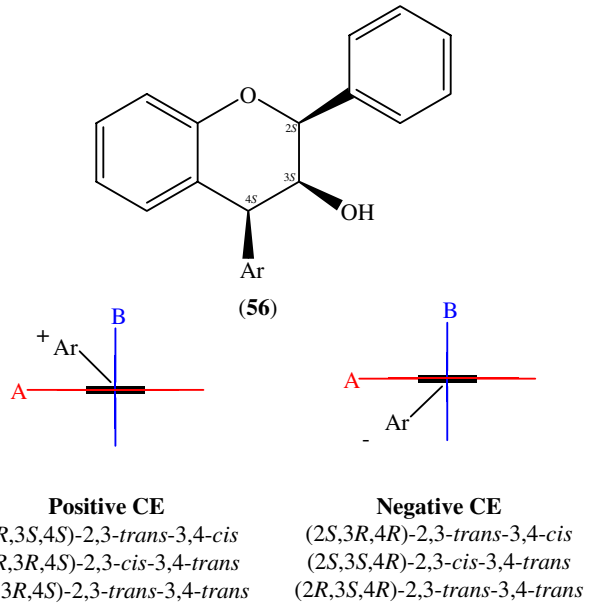


| Positive CE | Negative CE |
|---|---|
| (2*R*,3*S*,4*S*)-2,3-*trans*-3,4-*cis* | (2*S*,3*R*,4*R*)-2,3-*trans*-3,4-*cis* |
| (2*R*,3*R*,4*S*)-2,3-*cis*-3,4-*trans* | (2*S*,3*S*,4*R*)-2,3-*cis*-3,4-*trans* |
| (2*S*,3*R*,4*S*)-2,3-*trans*-3,4-*trans* | (2*R*,3*S*,4*R*)-2,3-*trans*-3,4-*trans* |

Fig. 51. The aromatic quadrant rule for 2,3-*trans*-3,4-*trans*-, 2,3-*trans*-3,4-*cis*-, and 2,3-*cis*-3,4-*trans*-4-arylflavan-3-ols.

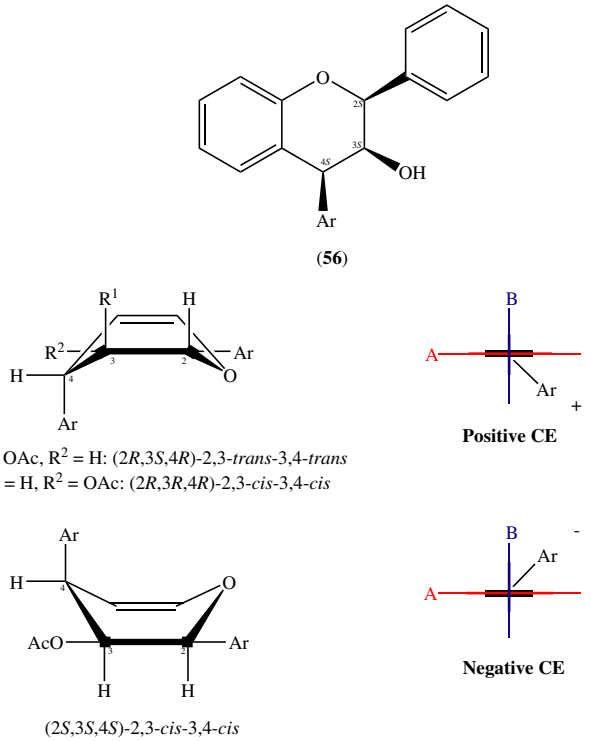


Fig. 52. Boat-conformations for 2,3-*cis*-3,4-*cis*-4-arylflavan-3-ols and the abnormal catechin-4α-phloroglucinol analogue.

sign of the high-amplitude CE and the sign of the aromatic quadrant of C4-aryl (Fig. 51).

For 2,3-*cis*-3,4-*cis*-4-arylflavan-3-ols and the abnormal catechin-4α-phloroglucinol analogue, the predicted and experimental CEs were originally correlated for boat-conformations (Fig. 52) (see also below for A ↔ E conformational itinerary). The compounds requiring a boat-conformation all have a 5-methoxysubstituent, reducing the non-bonding interaction between the C4-aryl and 5-methoxy groups, and between C3-acetyl and both C2- and C4-aryl groups (Van der Westhuizen et al., 1981).

The sign of the CE of 4-arylflavan-3-ols is principally determined by the spatial orientation and conformation of the *O*-heterocycle, and therefore minor deviations in orientation near the chiral centre may largely influence the amplitude and sign of the CE.

The enantiomeric hexamethyl ether 3-acetate of all-*trans*-4-arylflavan-3-ols (**59**) and (**60**) (Figs. 53 and 54) exhibit coupling constants of heterocyclic protons ($J_{2,3}$ 5.5, $J_{3,4}$ 4.5 Hz) characteristic of 5-oxygenated analogues with a C4-resorcinol-type substituent (Steynberg et al., 1988a,b,c, 1989; Van der Westhuizen et al., 1981; Botha et al., 1981b; Clark-Lewis, 1968; Fletcher

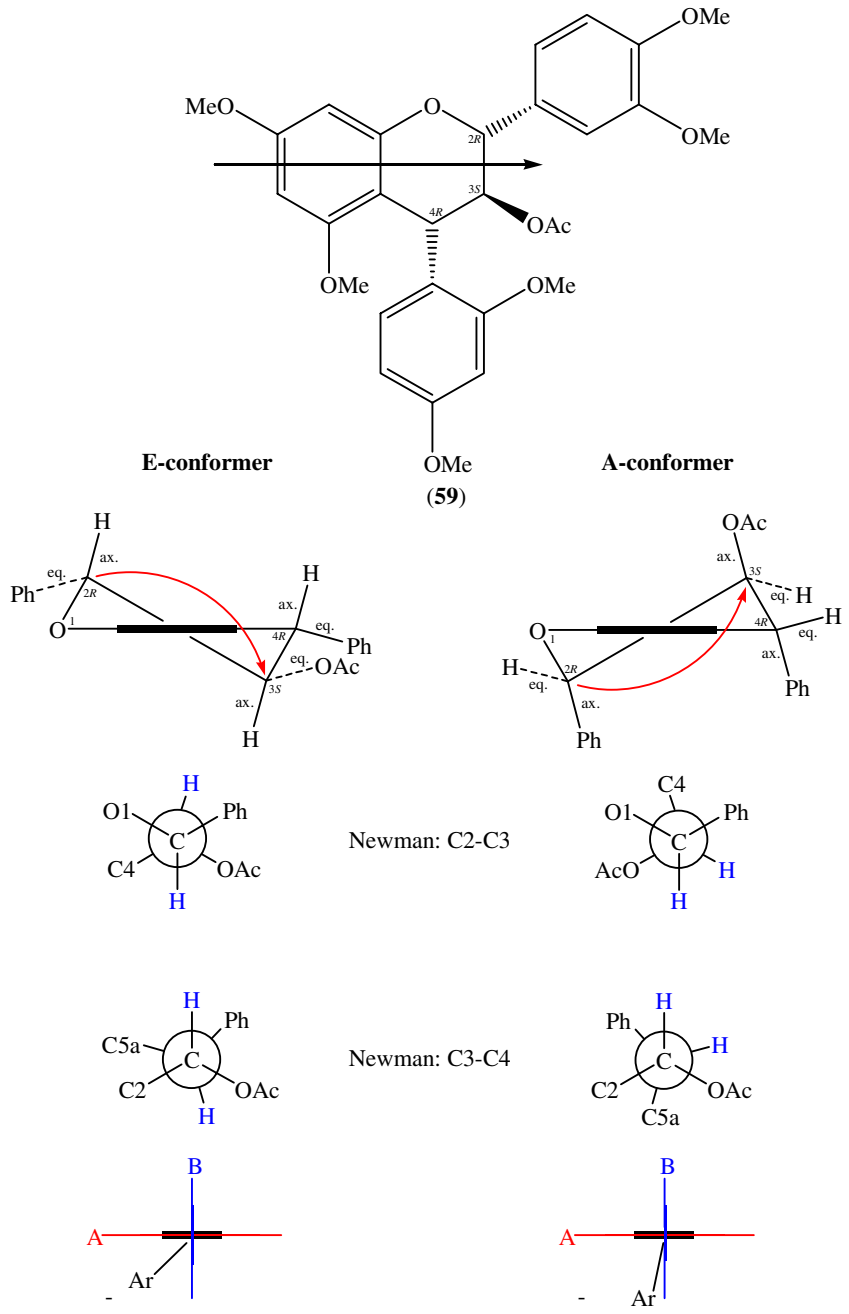


Fig. 53. Hexamethyl ether 3-acetate of (2*R*,3*S*,4*R*)-2,3-*trans*-3,4-*trans*-4-arylflavan-3-ol (**59**).

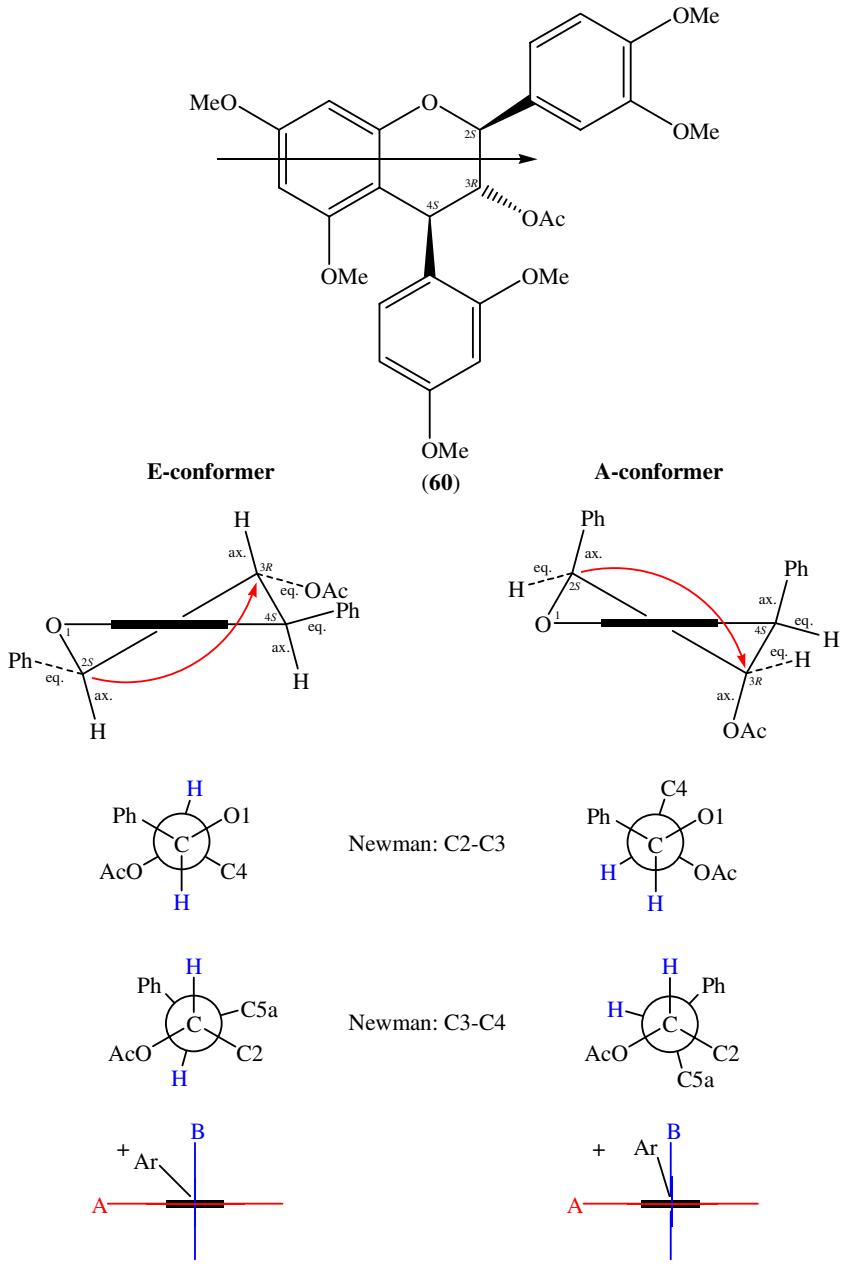


Fig. 54. Hexamethyl ether 3-acetate of (2*S*,3*R*,4*S*)-2,3-*trans*-3,4-*trans*-4-arylflavan-3-ol (**60**).

et al., 1977; Weinges et al., 1970). The small *J*-values reflect significant contributions of A-conformers, thereby reducing the dihedral angles of heterocyclic protons (Figs. 53 and 54; Porter et al., 1986). This may explain the reversal of the sign of the low-wavelength CE for these compounds, that is, a positive CE (Fig. 53) and a negative CE (Fig. 54), compared to the inverse effects predicted by the aromatic quadrant rule.

Conformational analysis of a series of 4-(2,4-dihydroxyphenyl)-5- oxyflavan-3-ols derivatives revealed that while the 2,4-*trans*-analogues displayed $^{1}$H NMR coupling constants expected for the relative configuration of the C-ring, coupling constants for analogues with a 2,4-*cis*-arrangement are abnormal (Steynberg et al., 1991). This also leads to a reversal of the CEs in the 230–240 nm region compared to the predicted aromatic quadrant rule CEs for half-chair/sofa conformations of the C-ring. Although this can be explained using boat conformations of the C-ring, the high strain-energy associated with this leads to the consideration of significant A-conformer contributions. The A-conformer represents a half-chair/sofa conformation for the pyran C-ring in which the C2-aryl group has an axial in stead of the normal equatorial orientation (Fig. 55). This mu-

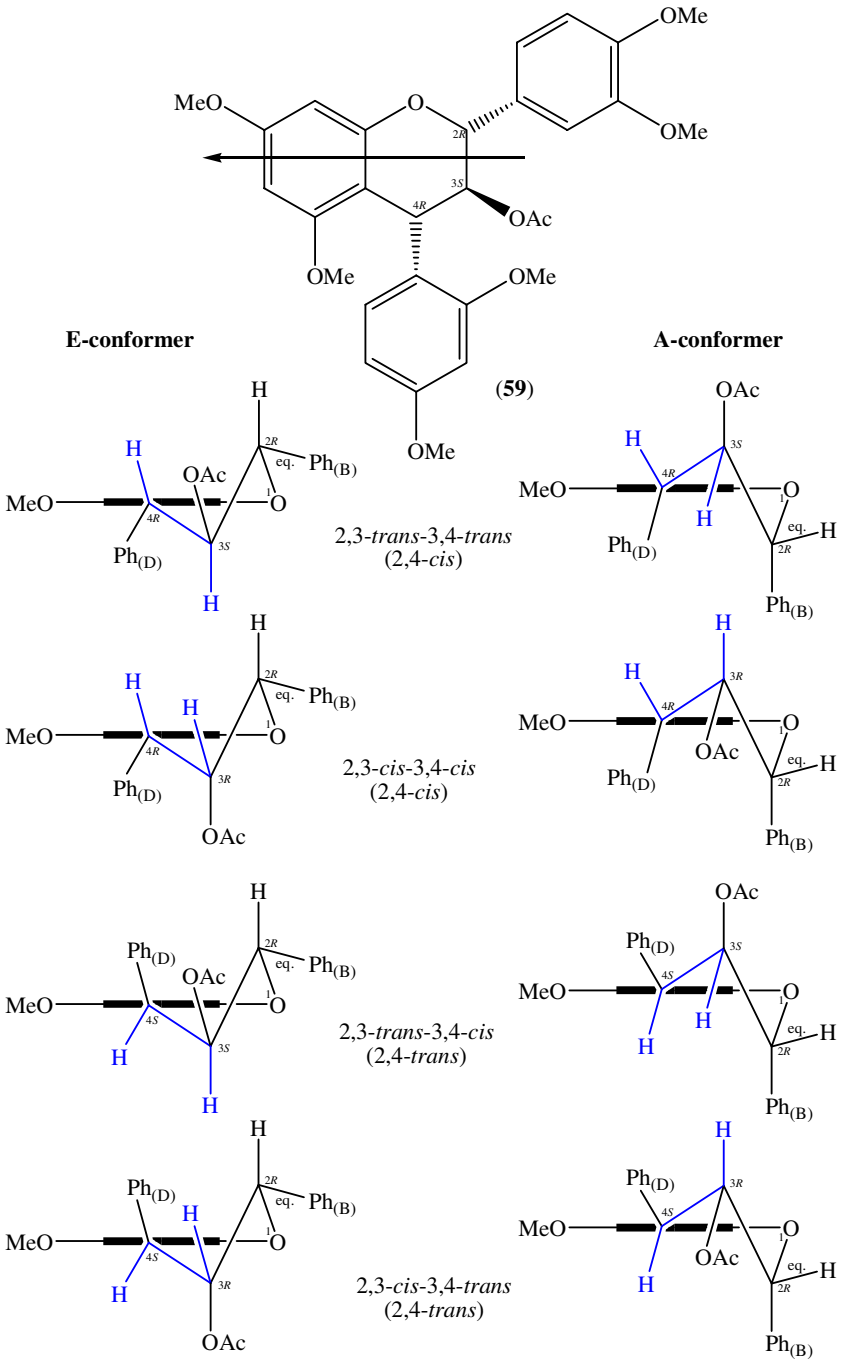


Fig. 55. E- and A-conformations. H3–C3–C4–H4 angles indicated in blue.

tates the dihedral angle between the heterocyclic protons and consequently the observed physical data.

The results of the conformational analysis (Steynberg et al., 1991) indicated pronounced contributions by A-conformers for isomers with a 2,4-*cis*-relative configuration as compared to 2,4-*trans*-isomers. This is presumably the result of several conducive factors including major contributions by 1,3-allylic strain (A-strain) between C5–OMe and the D-ring in the 2,4-*cis*-E-conformers (Johnson, 1968).

A half-chair conformation of the C-ring of 2,4-*trans*-E-conformers suggests quasi-axial 4β-substituents for the C-ring relative to the plane of the A-ring, accommodating C5–OMe more readily and therefore experiencing less A-strain than the 2,4-*cis*-E-conformers with their quasi-equatorial 4α-substituents. Maximum relief from 2,4-*cis*-A-strain is achieved by inversion of the pyran ring to an A-conformer (half-chair), locating C4-α-aryl in a quasi-axial orientation relative to the A-ring. By contrast, 2,4-*trans*-A-conformers possess C4-β-aryl in a

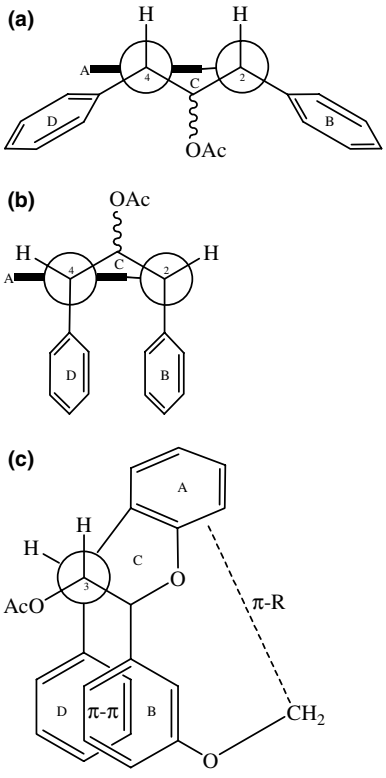


Fig. 56. 2,4-*cis*-4-Resorcyl-5-oxyflavan-4-ols. (a) A-conformer viewed along the C2–O1 and C4–C5a bonds, (b) E-conformer viewed along the C2–O1 and C4–C5a bonds, and (c) A-conformer viewed along the C3–C4 bond.

quasi-equatorial orientation resulting in greater A-strain and less stability (Fig. 55; Steynberg et al., 1991).

The 5-deoxy analogues do not show these irregularities regarding $^1$H NMR and CD data, indicating the predominance of the E-conformers and the absence of A-strain for both 2,4-*trans*- and 2,4-*cis*-isomers (Van der Westhuizen et al., 1981).

Although 1,3-diaxial arrangements are generally avoided on energetic grounds in terms of a classical stereochemical approach, the stability of A- [Fig. 56(b)] relative to E-conformers [Fig. 56(a)] for the 2,4-*cis*-isomers appears to be an exception by virtue of the aromaticity and associated geometry of the diaxial 2,4-biphenyl substituents, which are stacked parallel to the O1–C2 bond. This geometry also conforms to an offset face-to-face arrangement [Fig. 56(c)] required for π-stacking, i.e., stabilizing $\pi-\sigma$ attraction (Hunter and Sanders, 1990). This is probably further reinforced by a π–CH-interaction between C3″–OMe and the π-system of the A-ring [Fig. 56(c); Nishio and Hirota, 1989].

Van Zyl et al. (1993) synthesized a series free phenolic 4-arylflavan-3-ols consisting of four sets (3′,4′,5,7-tetrahydroxyflavan-3-ol or its 5-deoxy analogue coupled to phloroglucinol or resorcinol), each composed of three diastereomers (2,3-*trans*-3,4-*trans*, 2,3-*trans*-3,4-*cis* and 2,3-*cis*-3,4-*trans*). The low-wavelength (220–240 nm) negative CEs of the (2*R*,3*S*)-2,3-*trans*-3,4-*trans*-isomers are in agreement with an α-location of the D-ring, but is the reverse of what is found for the permethyl ether acetates. The (2*R*,3*S*)-2,3-*trans*-3,4-*cis*- and (2*R*,3*R*)-2,3-*cis*-3,4-*trans*-isomers show similar but positive CEs, indicating a β-orientation of the D-ring. The (2*S*,3*S*)-2,3-*cis*-3,4-*trans*-isomers display negative CEs compatible with an α-location of the D-ring.

Gaffield et al. (1989) proposed a transition polarization diagram to account for the sign of the short-wavelength (190–215 nm) CD couplet of dimeric procyanidins. The transition moment vector in the phloroglucinol D-ring is directed along the C1 → C4 axis. If the transition moment vector in ring A is similarly directed, a polarization diagram results for the exciton-split $^1$B band as shown in Fig. 57. Utilization of such a polarization diagram for the 4β → phloroglucinol

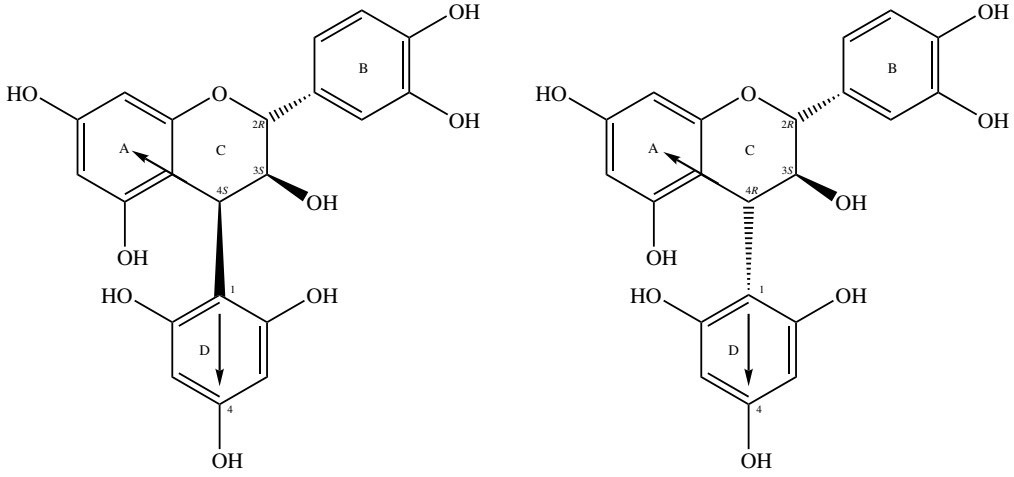


Fig. 57. Transition polarization diagram for 4-arylflavan-3-ols (**61**) and (**62**).

analogue (**61**) predicts positive chirality, in accordance with an observed positively signed couplet. Conversely, the left-handed screw pattern indicated for the electric transition dipole moment vectors for the 4α → phloroglucinol analogue (**62**) is reflected as a negative CD couplet.

The CD spectra of the 4-arylflavan-3-ols have served as reliable models for the interpretation of the CD data of dimeric proanthocyanidins of both the A- and B-types (Botha et al., 1981a).

## 14. Conclusion

Circular dichroism thus represents a powerful means of assessing the absolute configuration of the classes of naturally occurring monomeric flavonoids that possess stereocenters. It is a simple and straightforward technique involving non-expensive equipment, is non-destructive and requires ca. 1 mg of material. Thus, it is rather surprising that CD is not used routinely, perhaps as a result of the apparent simplicity yet often complicated interpretation of data?

## Acknowledgment

This work was supported in part by the United States Department of Agriculture, Agricultural Research Service Specific Cooperative Agreement, no. 58-6408-2-0009.

## References

Amschler, G., Frahm, A.W., Hatzelmann, A., Kilian, U., Müller-Doblies, D., Müller-Doblies, U., 1996. Constituents of *Veltheimia viridifolia*; I. Homoisoflavanones of the bulbs. Planta Medica 62, 534–539.

Antus, S., Snatzke, G., Steinke, I., 1983. Circular dichroism. LXXXI. Synthesis and circular dichroism of steroids with an isochromanone chromophore. Liebigs Annalen der Chemie 12, 2247–2261.

Antus, S., Baitz-Gács, E., Snatzke, G., Tóth, T.S., 1991. Synthesis and circular dichroism of steroids with a 1,4-benzodioxane chromophore: on the absolute configuration of (−)-silandrin. Liebigs Annalen der Chemie 7, 633–641.

Antus, S., Baitz-Gács, E., Kajtár, J., Snatzke, G., Tökés, A.L., 1994. Circular dichroism and absolute configuration of aza- and thiaflavanones. Liebigs Annalen der Chemie 5, 497–502.

Antus, S., Kurtán, T., Juhász, L., Kiss, L., Hollósi, M., Májer, Z.S., 2001. Chiroptical properties of 2,3-dihydrobenzo[*b*]furan and chromane chromophores in naturally occurring *O*-heterocycles. Chirality 13, 493–506.

Baig, M.I., Clark-Lewis, J.W., Thompson, M.J., 1969a. Flavan derivatives. XXVII. Synthesis of a new racemate of leucocyanidin tetramethyl ether (2,3-*cis*-3,4-*trans*-isomer): NMR spectra of the four racemates of leucocyanidin tetramethyl ether (5,7,3′,4′-tetramethoxyflavan-3,4-diol). Australian Journal of Chemistry 22, 2645–2650.

Baig, M.I., Clark-Lewis, J.W., Jemison, R.W., Thompson, M.J., 1969b. Four racemates of leucocyanidin tetramethyl ether (5,7,3′,4′-tetramethoxyflavan-3,4-diol). Journal of the Chemical Society, Chemical Communications 14, 820–821.

Barrett, M.W., Klyne, W., Scopes, P.M., Fletcher, A.C., Porter, L.J., Haslam, E., 1979. Plant proanthocyanidins. Part 6. Chiroptical studies. Part 95. Circular dichroism of procyanidins. Journal of the Chemical Society, Perkin Transactions 1, 2375–2377.

Barry, J., Kagan, H.B., Snatzke, G., 1971. Synthesis of the optically active methyl-1-tetralones and methyltetralins. Conformational studies by circular dichroism. Tetrahedron 27, 4737–4748.

Begley, M.J., Crombie, L., Whiting, D.A., 1975. Conformation and absolute configuration of rotenone. Examination of 8-bromorotenone by X-ray methods. Journal of the Chemical Society, Chemical Communications 20, 850–851.

Begley, M.J., Crombie, L., Hadi, A.H.B.A., Josephs, J.L., 1989. Synthesis of novel labile rotenoids with unnatural *trans*-B/C ring systems. Journal of the Chemical Society, Perkin Transactions 1: Organic and Bio-Organic Chemistry 1, 204–205.

Bekker, R., Li, X.C., ElSohly, H.N., Clark, A.M., Brandt, E.V., Ferreira, D., 2001. Resolution and absolute configuration of naturally occurring auronols. Journal of Natural Products 64, 345–347.

Bognár, R., Clark-Lewis, J.W., Tökés, A.L., Rákosi, M., 1970. Resolution of 4- aminoflavan into its optical isomers – nuclear magnetic resonance spectra of 4-aminoflavan and 3-aminoflavanone derivatives. Australian Journal of Chemistry 23, 2015–2025.

Bohm, B.A., 1998. Introduction to Flavonoids. Harwood Academic Publishers, Australia, pp. 80–112.

Bolger, B.H., Hirwe, A., Marathe, K.G., Philbin, E.M., Vickars, M.A., Lillya, C.P., 1966. Nuclear magnetic resonance spectra and stereochemistry of 4-substituted flavans. Tetrahedron 22, 621–628.

Botha, J.J., Ferreira, D., Roux, D.G., 1978. Condensed tannins. Circular dichroism method of assessing the absolute configuration at carbon-4 of 4-arylflavan-3-ols, and stereochemistry of their formation from flavan-3,4-diols. Journal of the Chemical Society, Chemical Communications 16, 698–700.

Botha, J.J., Ferreira, D., Roux, D.G., 1981a. Synthesis of condensed tannins. Part 4. A direct biomimetic approach to [4 → 6]- and [4 → 8]-biflavanoids. Journal of the Chemical Society, Perkin Transactions 1, 1235–1245.

Botha, J.J., Young, D.A., Ferreira, D., Roux, D.G., 1981b. Synthesis of condensed tannins. Part 1. Stereoselective and stereospecific syntheses of optically pure 4-arylflavan-3-ols, and assessment of their absolute stereochemistry at C-4 by means of circular dichroism. Journal of the Chemical Society, Perkin Transactions 1, 1213–1219.

Büchi, G., Crombie, L., Godin, P.J., Kaltenbronn, J.S., Siddalingaiah, K.S., Whiting, D.A., 1961. The absolute configuration of rotenone. Journal of the Chemical Society, Abstracts, 2843–2860.

Cahn, R.S., Ingold, C.K., Prelog, V., 1956. Specification of asymmetric configuration in organic chemistry. Experientia 12, 81–94.

Cahn, R.S., Ingold, C.K., Prelog, V., 1966. Specification of molecular chirality. Angewandte Chemie, International Edition in English 54, 385–415.

Calzada, F., Cerda-Garcá-Rojas, C.M., Meckes, M., Cedillo-Rivera, R., Bye, R., Mata, R., 1999. Geranins A and B, new antiprotozoal A-type proanthocyanidins from *Geranium niveum*. Journal of Natural Products 62, 705–709.

Carlson, D.G., Weisleder, D., Tallent, W.H., 1973. NMR investigations of rotenoids. Tetrahedron 29, 2731–2741.

Chen, H.F., Tanaka, T., Nonaka, G.I., Fujioka, T., Mihashi, K., 1993. Tannins and related compounds. Part 121. Phenylpropanoid-substituted catechins from *Castanopsis hystrix* and structure revision of cinchonains. Phytochemistry 33, 183–187.

Clark-Lewis, J.W., 1962. Configurations of optically active flavonoid compounds. Reviews of Pure and Applied Chemistry 12, 96–116.

Clark-Lewis, J.W., 1968. Flavan derivatives. XXI. Nuclear magnetic resonance spectra, configuration, and conformation of flavan derivatives. Australian Journal of Chemistry 21, 2059–2075.

Clark-Lewis, J.W., Williams, L.R., 1967. Flavan derivatives. XVII. Epimerization of the benzylic 4-hydroxyl group in flavan-3,4-diols and the formation of 4-alkyl ethers by solvolysis. Australian Journal of Chemistry 20, 2151–2167.

Clark-Lewis, J.W., Jackman, L.M., Spotswood, T.M., 1964. Nuclear magnetic resonance (NMR) spectra, stereochemistry, and conformation of flavan derivatives. Australian Journal of Chemistry 17, 632–648.

Clark-Lewis, J.W., Dainis, I., Ramsay, G.C., 1965. Flavan derivatives. XIV. The absolute configuration of some 1,2-diarylpropane derivatives and of some isoflavans. Australian Journal of Chemistry 18, 1035–1048.

Cook, J.T., Ollis, W.D., Sutherland, I.O., Gottlieb, O.R., 1978. Isoflavonoid constituents of *Dalbergia* and *Machaerium* species. Part 5. Pterocarpans from *Dalbergia spruceana*. Phytochemistry 17, 1419–1422.

Crabbé, P., 1965. Optical Rotatory Dispersion and Circular Dichroism in Organic Chemistry. Holden-Day, San Francisco.

Crabbé, P., 1967a. An introduction to optical rotatory dispersion and circular dichroism in organic chemistry. In: Snatzke, G. (Ed.), Optical Rotatory Dispersion and Circular Dichroism in Organic Chemistry. Heyden and Son Limited, London, pp. 2–10.

Crabbé, P., 1967b. Recent applications of optical rotatory dispersion and optical circular dichroism in organic chemistry. In: Allinger, N.L., Eliel, E.L. (Eds.), Topics in Stereochemistry, vol. 1. Wiley, New York, London and Sydney, pp. 93–185.

Crombie, L., Lown, J.W., 1961. Determination of the geometry of the B/C fusion of rotenoids by means of long-range asymmetric magnetic shielding of the carbonyl group, London. Proceedings of the Chemical Society, 299–300.

Crombie, L., Lown, J.W., 1962. Proton magnetic studies (NMR) of rotenone and related compounds. Journal of the Chemical Society, Abstracts, 775–781.

DeAngelis, G.G., Wildman, W.C., 1969. Circular dichroism studies. I. A quadrant rule for the optically active aromatic chromophore in rigid polycyclic systems. Tetrahedron 25, 5099–5112.

Dewick, P.M., 1982. Isoflavonoids. In: Harborne, J.B., Mabry, T.J. (Eds.), The Flavonoids: Advances in Research. Chapman and Hall Ltd., London, pp. 535–640.

Dewick, P.M., 1988. Isoflavonoids. In: Harborne, J.B. (Ed.), The Flavonoids: Advances in Research Since 1980. Chapman and Hall Ltd., London, pp. 125–210.

Dewick, P.M., 1994. Isoflavonoids. In: Harborne, J.B. (Ed.), The Flavonoids: Advances in Research Since 1986. Chapman and Hall Ltd., London, pp. 117–238.

Djerassi, C., 1967. The role of optical rotatory dispersion and circular dichroism in organic chemistry – origin, present development and future prospects. In: Snatzke, G. (Ed.), Optical Rotatory Dispersion and Circular Dichroism in Organic Chemistry. Heyden and Son Limited, London, pp. 16–17.

Djerassi, C., Ollis, W.D., Russell, R.C., 1961. Optical rotatory dispersion studies. XXXVIII. Relative stereochemistry of the rotenoids. Journal of the Chemical Society, Abstracts, 1448–1453.

Donnelly, D.M.X., Boland, G., 1994. Neoflavonoids. In: Harborne, J.B. (Ed.), The Flavonoids: Advances in Research Since 1986. Chapman and Hall Ltd., London, pp. 239–258.

Donnelly, D.M.X., Keenan, P.J., Prendergast, J.P., 1973. Isoflavonoids of *Dalbergia ecastophyllum*. Phytochemistry 12, 1157–1161.

Dornhege, E., Snatzke, G., 1970. Circular dichroism. XL. Chiroptic properties of amino indanols and related compounds. Tetrahedron 26, 3059–3067.

Dumontet, V., Van Hung, N., Adeline, M.T., Riche, C., Chiaroni, A., Svenet, T., Guritte, F., 2004. Cytotoxic flavonoids and α-pyrones from *Cryptocarya obovata*. Journal of Natural Products 67, 858–862.

Eliel, E.L., Allinger, N.L., Angyal, S.J., Morrison, G.A., 1965. Conformational Analysis. Wiley, New York.

Emsley, J.W., Feeney, J., Sutcliffe, L.H., 1968. High Resolution Nuclear Magnetic Resonance Spectroscopy. Pergamon Press, Oxford, New York, pp. 166–170.

Fan, W., Tezuka, Y., Xiong, Q., Hattori, M., Namba, T., Kadota, S., 1999. Apocynins A–D: new phenylpropanoid-substituted flavan-3-ols isolated from leaves of *Apocynum venetum* (Luobuma-ye). Chemical & Pharmaceutical Bulletin 47, 1049–1050.

Ferreira, D., Nel, R.J.J., Bekker, R., 1999. Condensed tannins. In: Pinto, B.M. (Ed.), Comprehensive Natural Products Chemistry, vol. 3. Elsevier, New York, pp. 747–797.

Ferreira, D., Marais, J.P.J., Slade, D., Walker, L.A., 2004. Circular dichroic properties of flavan-3,4-diols. Journal of Natural Products 67, 174–178.

Fletcher, A.C., Porter, L.J., Haslam, E., Gupta, R.K., 1977. Plant proanthocyanidins. Part 3. Conformational and configurational studies of natural procyanidins. Journal of the Chemical Society, Perkin Transactions 1, 1628–1637.

Foo, L.Y., 1987. Phenylpropanoid derivatives of catechin, epicatechin and phylloflavan from *Phyllocladus trichomanoides*. Phytochemistry 26, 2825–2830.

Foo, L.Y., 1989. Flavanocoumarins and flavanophenylpropanoids from *Phyllocladus trichomanoides*. Phytochemistry 28, 2477–2481.

Friedrich, W., Galensa, R., 2002. Identification of a new flavanol glucoside from barley (*Hordeum vulgare* L.) and malt. European Food Research and Technology 214, 388–393.

Friedrichsen, W., Schöning, A., 1990. The stereochemistry of *cis*-pterocarpans. A theoretical study. Zeitschrift fuer Naturforschung, Chemical Sciences 45, 1049–1054.

Fukami, H., Nakajima, M., 1971. In: Jacobson, M., Crosby, D.G. (Eds.), Naturally Occurring Insecticides. Marcel Dekker, New York, p. 71.

Gaffield, W., 1970. Circular dichroism, optical rotatory dispersion and absolute configuration of 3-hydroxyflavanones and their glycosides. Determination of aglycone chirality in flavanone glycosides. Tetrahedron 26, 4093–4108.

Gaffield, W., Foo, L.Y., Porter, L.J., 1989. Exciton split Cotton effect of dimeric procyanidins. Journal of Chemical Research, (S), 144–145.

Galeffi, C., Rasoanaivo, P., Federici, E., Palazzino, G., Nicoletti, M., Rasolondratovo, B., 1997. Two prenylated isoflavanones from *Millettia pervilleana*. Phytochemistry 45, 189–192.

Garo, E., Wolfender, J.L., Hostettmann, K., Hiller, W., Antus, S., Mavi, S., 1998. Prenylated flavanones from *Monotes engleri*: Online structure elucidation by LC/UV/NMR. Helvetica Chimica Acta 81, 754–763.

Hagishita, S., Kuriyama, K., 1982. Confirmation of the sector rule of the benzenoid chromophore. Bulletin of the Chemical Society of Japan 55, 3216–3224.

Hamburger, M.O., Cordell, G.A., Ruangrungsi, N., Tantivatana, P., 1988. Traditional medicinal plants of Thailand. 10. Candenatone, a novel purple pigment from *Dalbergia candenatensis*. Journal of Organic Chemistry 53, 4161–4165.

Haslam, E., 1982. Proanthocyanidins. In: Harborne, J.B., Mabry, T.J. (Eds.), The Flavonoids: Advances in Research. Chapman and Hall Ltd., London, p. 421.

Harada, N., Nakanishi, K., 1983. Circular Dichroic Spectroscopy. Exciton Coupling in Organic Stereochemistry. University Science Books, Mill Valley, CA.

Johnson, F., 1968. Allylic strain in six-membered rings. Chemical Reviews (Washington, DC) 68, 375–413.

Hunter, C.A., Sanders, J.K.M., 1990. The nature of π–π interactions. Journal of the American Chemical Society 112, 5525–5534.

Kiss, L., Kurtán, T., Antus, S., Bényei, A., 2003. Chiroptical properties and synthesis of enantiopure *cis* and *trans* pterocarpan skeleton. Chirality 15, 558–563.

Kolodziej, H., 1983. The first naturally occurring 4-arylflavan-3-ol. Tetrahedron Letters 24, 1825–1828.

Kolodziej, H., 1984. Occurrence of procyanidins in *Nelia meyeri*. Phytochemistry 23, 1745–1752.

Korver, O., Wilkins, C.K., 1971. Circular dichroism spectra of flavanols. Tetrahedron 27, 5459–5465.

Kostova, I., Berova, N., Ivanov, P., Mikhova, B., Rakovska, R., 1991. Stereochemical studies of some 12a-substituted rotenoid derivatives. Croatica Chemica Acta 64, 637–647.

Kurosawa, K., Ollis, W.D., Redman, B.T., Sutherland, I.O., 1968. Absolute configurations of the animal metabolite, equol, three naturally occurring isoflavans, and one natural isoflavanquinone. Chemical Communications 20, 1265–1267.

Kurosawa, K., Ollis, W.D., Redman, B.T., Sutherland, I.O., Alves, H.M., Gottlieb, O.R., 1978. Isoflavonoid constituents of *Dalbergia* and *Machaerium* species. Part 6. Absolute configurations of isoflavans. Phytochemistry 17, 1423–1426.

Kurtán, T., Baitz-Gács, E., Májer, Z., Antus, S., 2000. Synthesis and circular dichroism of steroids with 2,3-dihydro-1-benzofuran and 4*H*-benzopyran chromophores; revision of the absolute configuration of some norneolignans from *Krameria cystisoides*. Journal of the Chemical Society, Perkin Transactions 1, 453–461.

Lami, N., Kadota, S., Tezuka, Y., Kikuchi, T., 1990. Constituents of the roots of *Boerhaavia diffusa* L. II. Structure and stereochemistry of a new rotenoid, boeravinone C. Chemical & Pharmaceutical Bulletin 38, 1558–1562.

Lévai, A., 1998. Utilization of the chiroptical spectroscopies for the structure elucidation of flavonoids and related benzopyran derivatives. Acta Chimica Slovenica 45, 267–284.

Li, X.C., Joshi, A.S., Tan, B., ElSohly, H.N., Walker, L.A., Zjawiony, J.K., Ferreira, D., 2002. Absolute configuration, conformation, and chiral properties of flavanone-(3 → 8″)-flavone biflavonoids from *Rheedia acuminata*. Tetrahedron 58, 8709–8717.

Lightner, D.A., 2000. The Octant Rule. In: Berova, N., Nakanishi, K., Woody, R.W. (Eds.), Circular Dichroism – Principles and Applications. Wiley, New York, p. 261.

Luche, M.J., Marquet, A., Snatzke, G., 1972. Absolute configuration of 1-indanones and 2-substituted 1-tetralones. Tetrahedron 28, 1677–1695.

Majer, Z., Hollósi, M., Lévai, A., Majerić, M., Šunjić, V., 1995. CD spectroscopic study of absolute conformation and configuration of some 4-hydroxychromans. Spectroscopy Letters 28, 1181–1190.

Mayer, R., 2004. Five biflavonoids from *Calycopteris floribunda* (Combretaceae). Phytochemistry 65, 593–601.

Moffitt, W., Woodward, R.B., Moscowitz, A., Klyne, W., Djerassi, C., 1961. Structure and the optical rotatory dispersion of saturated ketones. Journal of the American Chemical Society 83, 4013–4018.

Moscowitz, A., 1961. Applications of the Kronig–Kramers theorem to optical activity. Tetrahedron 13, 48–56.

Nel, R.J.J., Van Rensburg, H., Van Heerden, P.S., Ferreira, D., 1999. Stereoselective synthesis of flavonoids. Part 8. Free phenolic flavan-3-ol diastereoisomers. Journal of Chemical Research, (S) 606–607 (M), 2610–2625.

Nishio, M., Hirota, M., 1989. CH/π interaction: implications in organic chemistry. Tetrahedron 45, 7201–7245.

Nonaka, G., Nishioka, I., 1982. Tannins and related compounds. VII. Phenylpropanoid-substituted epicatechins, cinchonains from *Cinchona succirubra*. Chemical & Pharmaceutical Bulletin 30, 4268–4276.

Nonaka, G.I., Goto, Y., Kinjo, J., Nohara, T., Nishioka, I., 1987. Tannins and related compounds. LII. Studies on the constituents of the leaves of *Thujopsis dolabrata* SIEB. *et* ZUCC. Chemical & Pharmaceutical Bulletin 35, 1105–1108.

Oberholzer, M.E., Rall, G.J.H., Roux, D.G., 1974. Concurrence of 12a-hydroxy- and 12a-*O*-methylrotenoids. Isolation of the first natural 12a-*O*-methylrotenoids. Tetrahedron Letters 25, 2211–2214.

Ollis, W.D., Rhodes, C.A., Sutherland, I.O., 1967. The extractives of *Millettia dura* (Dunn). The constitutions of durlettone, durmillone, milldurone, millettone and millettosin. Tetrahedron 23, 4741–4760.

Pachler, K.G.R., Underwood, W.G.E., 1967. Proton magnetic resonance study of some pterocarpan derivatives. The conformation of the 6a,11a-dihydro-6*H*-benzofuro[3,2-*c*][1]benzopyran ring system. Tetrahedron 23, 1817–1826.

Paiva, N.L., Sun, Y., Dixon, R.A., VanEtten, H.D., Hrazdina, G., 1994. Molecular cloning of isoflavone reductase from pea (*Pisum sativum* L.): evidence for a 3*R*-isoflavanone intermediate in (+)-pisatin biosynthesis. Archives of Biochemistry and Biophysics 312, 501–510.

Pelter, A., Amenechi, P.I., 1969. Isoflavonoid and pterocarpinoid extractives of *Lonchocarpus laxiflorus*. Journal of the Chemical Society 6, 887–896.

Petruska, J., 1961. Changes in the electronic transitions of aromatic hydrocarbons on chemical substitution. II. Application of perturbation theory to substituted-benzene spectra. Journal of Chemical Physics 34, 1120–1136.

Platt, J.R., 1949. Classification of spectra of cata-condensed hydrocarbons. Journal of Chemical Physics 17, 484–495.

Platt, J.R., 1951. Spectroscopic moment: a parameter of substituent groups determining aromatic ultraviolet intensities. Journal of Chemical Physics 19, 263–271.

Porter, L.J., 1988. Flavans and proanthocyanidins. In: Harborne, J.B. (Ed.), The Flavonoids – Advances in Research Since 1980. Chapman and Hall Ltd., London and New York, p. 27.

Porter, L.J., Wong, R.Y., Benson, M., Chan, B.G., Vishwanadhan, V.N., Gandour, R.D., Mattice, W.L., 1986. Conformational analysis of flavans: proton NMR and molecular mechanical (MM2) studies of the benzpyran ring of 3′,4′,5,7-tetrahydroxyflavan-3-ols: the crystal and molecular structure of the procyanidin (2*R*,3*S*,4*R*)-3′,4′,5,7-tetramethoxy-4-(2,4,6-trimethoxyphenyl)flavan-3-ol. Journal of Chemical Research, (*S*) 86-87, (*M*) 0830.

Quaglia, M.G., Desideri, N., Bossù, E., Melchiorre, P., Conti, C., 1991. Enantiomeric separation of substituted flavanoids by LC-DAD. Journal of Pharmaceutical and Biomedical Analysis 9, 811–815.

Russell, G.B., 1997. New isoflavonoids from root bark of kowhai (*Sophora microphylla*). Australian Journal of Chemistry 50, 333–336.

Santos, A.S., Caetano, L.C., Sant'Ana, A.E.G., 1998. A 12a-hydroxyrotenoid from roots of *Boerhaavia coccinea*. Phytochemistry 49, 255–258.

Sashida, Y., Yamamoto, T., Koike, C., Shimomura, H., 1976. The chemical constituents of santalaceae. Part 1. A new flavan glycoside from *Buckleya lanceolata* leaves. Phytochemistry 15, 1185–1186.

Schulte, J., Snatzke, G., 1989. Circular dichroism. XCII. Proof of the sector rule for α-band CD of the *O*-dialkyl-substituted benzene chromophore. Chemische Berichte 122, 1373–1374.

Schöning, A., Friedrichsen, W., 1989. The stereochemistry of pterocarpanoids. A theoretical study. Zeitschrift fuer Naturforschung B 44, 975–982.

Shawl, A.S., Mengi, N., Misra, L.N., Vishwapaul, 1988. Irispurinol, a 12a-hydroxyrotenoid from *Iris spuria*. Phytochemistry 27, 3331–3332.

Snatzke, G., 1965a. Circular dichroism. VIII. Modification of the octant rule for α,β-unsaturated ketones – theory. Tetrahedron 21, 413–419.

Snatzke, G., 1965b. Circular dichroism. X. Modification of the octant rule for α,β-unsaturated ketones – cisoid enones, dienones, and aryl ketones. Tetrahedron 21, 439–448.

Snatzke, G., Ho, P.C., 1971. Circular dichroism. XLVI. Rules for benzene Cotton-effects. Tetrahedron 27, 3645–3653.

Snatzke, G., Kajtár, M., Werner-Zamojska, F., 1972. Circular dichroism. XLVII. Influence of substitution pattern on the benzene $^1L_b$-band Cotton effect. Tetrahedron 28, 281–288.

Snatzke, G., Znatzke, F., Tökés, A.L., Rákosi, M., Bognár, R., 1973a. Flavonoids. XXVIII. Circular dichroism. LXI. Chiroptical properties of 4-substituted flavans. Tetrahedron 29, 909–912.

Snatzke, G., Kajtár, M., Snatzke, F., 1973b. Aromatic chromophores. In: Ciardelli, F., Salvadori, P. (Eds.), Fundamental Aspects and Developments in Optical Rotatory Dispersion and Circular Dichroism. Heyden & Son Ltd., London, pp. 148–172.

Steynberg, J.P., Burger, J.F.W., Young, D.A., Brandt, E.V., Steenkamp, J.A., Ferreira, D., 1988a. Novel base-catalyzed rearrangements of (−)-fisetinidol-(+)-catechin profisetinidins with 2,3-*trans*-3,4-*cis*-flavan-3-ol constituent units. Journal of the Chemical Society, Chemical Communications 15, 1055–1057.

Steynberg, J.P., Burger, J.F.W., Young, D.A., Brandt, E.V., Steenkamp, J.A., Ferreira, D., 1988b. Oligomeric flavanoids. Part 3. Structure and synthesis of phlobatannins related to (−)-fisetinidol-(4α,6) and (4α,8)-(+)-catechin profisetinidins. Journal of the Chemical Society, Perkin Transactions 1, 3323–3329.

Steynberg, J.P., Burger, J.F.W., Young, D.A., Brandt, E.V., Steenkamp, J.A., Ferreira, D., 1988c. Oligomeric flavanoids. Part 4. Base-catalyzed conversions of (−)-fisetinidol-(+)-catechin profisetinidins with 2,3-*trans*-3,4-*cis*-flavan-3-ol constituent units. Journal of the Chemical Society, Perkin Transactions 1, 3331–3338.

Steynberg, J.P., Burger, J.F.W., Young, D.A., Brandt, E.V., Ferreira, D., 1989. Oligomeric flavanoids. Part 6. Evidence supporting the inversion of absolute configuration at 3-C associated with base catalyzed A-/B-ring interchange of precursors having 2,3-*trans*-3,4-*cis*-flavan-3-ol constituent units. Heterocycles 28, 923–935.

Steynberg, J.P., Brandt, E.V., Ferreira, D., 1991. Conformational analysis of oligomeric flavanoids. Part 1. 4-Arylflavan-3-ols. Journal of the Chemical Society, Perkin Transactions 2, 1569–1573.

Strack, D., 1997. Phenolic metabolism. In: Dey, P.M., Harborne, J.B. (Eds.), Plant Biochemistry. Academic Press, London, pp. 387–416.

Suginome, H., 1966. Absolute and relative stereochemical correlation of isoflavanone, sophorol, and naturally occurring isoflavan derivatives. Bulletin of the Chemical Society of Japan 39, 1544–1547.

Szarvas, S.Z., Szókán, G.Y., Hollösi, M., Kiss, L., Antus, S., 2000. Determination of the absolute configuration of synthetic pterocarpans by chiral HPLC using on-line CD detection. Enantiomer 5, 535–543.

Tahara, S., Narita, E., Ingham, J.L., Mizutani, J., 1990. New rotenoids from the root bark of Jamaican dogwood (*Piscidia erythrina* L.). Zeitschrift fuer Naturforschung, C: Journal of Biosciences 45, 154–160.

Unai, T., Yamamoto, I., Cheng, H.M., Casida, J.E., 1973. Synthesis and stereochemical characterization of hydroxyl- and epoxy-derivatives of rotenone. Agricultural and Biological Chemistry 37, 387–401.

Van Aardt, T.G., Van Rensburg, H., Ferreira, D., 2001. Synthesis of isoflavonoids. Enantiopure *cis*- and *trans*-6a-hydroxypterocarpans and a racemic *trans*-pterocarpan. Tetrahedron 57, 7053–7235.

Van der Westhuizen, J.H., Ferreira, D., Roux, D.G., 1981. Synthesis of condensed tannins. Part 2. Synthesis by photolytic rearrangement, stereochemistry, and circular dichroism of the first 2,3-*cis*-3,4-*cis*-4-arylflavan-3-ols. Journal of the Chemical Society, Perkin Transactions 1, 1220–1226.

Van Rensburg, H., Steynberg, P.J., Burger, J.F.W., Van Heerden, P.S., Ferreira, D., 1999. Circular dichroic properties of flavan-3-ols. Journal of Chemical Research, 450–451.

Van Zyl, P.W., Steynberg, J.P., Brandt, E.V., Ferreira, D., 1993. Spectroscopic properties of free phenolic 4-arylflavan-3-ols as models for natural condensed tannins. Magnetic Resonance in Chemistry 31, 1057–1063.

Velluz, L., Legrand, M., Grosjean, M., 1965. Optical Circular Dichroism. Principles, Measurements, and Applications. Verlag Chemie, GMBH, Academic Press Inc., New York and London, pp. 5–182.

Verbit, L., Clark-Lewis, J.W., 1968. Optically active aromatic chromophores. VIII. The isoflavanoid and rotenoid series. Tetrahedron 24, 5519–5527.

Versteeg, M., Bezuidenhoudt, B.C.B., Ferreira, D., 1999. Stereoselective synthesis of isoflavonoids. (*R*)- and (*S*)-isoflavans. Tetrahedron 55, 3365–3376.

Weinges, K., Marx, H.D., Göritz, K., 1970. Proanthocyanidins. XV. Rotational hindrance at the $C(sp^2)$–$C(sp^3)$ linkage of the 4-aryl-substituted polymethoxyflavans. Chemische Berichte 103, 2336–2343.

Wong, E., 1975. The Isoflavonoids. In: Harborne, J.B., Mabry, T.J., Mabry, H. (Eds.), The Flavonoids. Chapman and Hall Ltd., London, pp. 743–800.

Woodward, M.D., 1980. Phaseollin formation and metabolism in *Phaseolus vulgaris*. Phytochemistry 19, 921–927.

Wu, T.S., Hsu, M.Y., Kuo, P.C., Sreenivasulu, B., Damu, A.G., Su, C.R., Li, C.Y., Chang, H.C., 2003. Constituents from the leaves of *Phellodendron amurense* var. *Wilsonii* and their bioactivity. Journal of Natural Products 66, 1207–1211.

Yahara, S., Saijo, R., Nohara, T., Konishi, R., Yamahara, J., Kawasaki, T., Miyahara, K., 1985. Novel bi-isoflavonoids from *Dalbergia odorifera*. Chemical & Pharmaceutical Bulletin 33, 5130–5133.

Yahara, S., Ogata, T., Saijo, R., Konishi, R., Yamahara, J., Miyahara, K., Nohara, T., 1989. Isoflavan and related compounds from *Dalbergia odorifera* I. Chemical & Pharmaceutical Bulletin 37, 979–987.

Yenesew, A., Midiwo, J.O., Waterman, P.G., 1998. Rotenoids, isoflavones and chalcones from the stem bark of *Millettia usaramensis* subspecies *usaramensis*. Phytochemistry 47, 295–300.

Yenesew, A., Derese, S., Midiwo, J.O., Oketch-Rabah, H.A., Lisgarten, J., Palmer, R., Heydenreich, M., Peter, M.G., Akala, H., Wangui, J., Liyala, P., Waters, N.C., 2003. Anti-plasmodial activities and X-ray crystal structures of rotenoids from *Millettia usaramensis* subspecies *usaramensis*. Phytochemistry 64, 773–779.

**Desmond Slade** graduated from the University of Stellenbosch, South Africa in 2000, where he obtained his PhD (Chemistry) on the chemical characterization of the interdigital secretion of the black wildebeest under the supervision of Prof. Ben V. Burger. He started as a Postdoctoral Research Associate at the National Center for Natural Products Research, University of Mississippi, at the end of 2000, working on the synthesis of antimalarial 8-amino-quinolines and the synthesis of buprenorphine-3-β-D-glucuronide and norbuprenorphine-3-β-D-glucuronide and their deuterated analogues under the supervision of Dr. Daneel Ferreira. Since 2003 he is an Associate Research Scientist in the Center where he is also involved in cannabinoid research.

**Daneel Ferreira** graduated from the University of Pretoria, South Africa in 1964. He completed the B.Sc. (Hons.) and M.Sc. programmes of the Chemistry Department, University of the Orange Free State, Bloemfontein, South Africa through part time studies. In 1969, he was appointed as Technical Assistant in the Chemistry Department at UOFS, obtained the D.Sc. degree in Organic Chemistry in 1973 and progressed to the ranks of Professor of Organic Chemistry in 1985. He spent 1977 as a Visiting Lecturer at Imperial College, London where he worked under the supervision of the late Sir Derek Barton. His main area of research is in the study of the chemistry of flavonoids and proanthocyanidins where he focusses on structure elucidation (up to the tetraflavanoid level) via physical methods, especially NMR and CD, semi-synthesis of oligomers, stereoselective syntheses of monomeric precursors, and the development of general methodologies to manipulate the molecular backbone of the $C_6 \cdot C_3 \cdot C_6$ unit. He was invited to establish a Research Unit for Polyphenol- and Synthetic Chemistry at UOFS by the Foundation for Research Development, Pretoria and was duly appointed as Director in 1990. He held this position until 1998 before joining the Thad Cochran National Center for Natural Products Research, University of Mississippi in 1999 as Visiting Scholar, and was promoted to Principal Scientist in 2000. He was offered the Chair of the Department of Pharmacognosy, University of Mississippi, in 2004 where he continues with research of the chemistry of Natural Products.

**Jannie P.J. Marais** studied at the University of the Free State, Bloemfontein, South Africa where he obtained his PhD in Organic Chemistry in 2002 under joint supervision of Prof. E.V. Brandt, Dr H. van Rensburg and Dr. D. Ferreira. His research work focused on characterization of the free phenolic profile of South African red wine, and the stereoselective synthesis of constituent flavonoids, e.g. flavan-3,4-diols and flavanones. He joined the National Center for Natural Products Research at the University of Mississippi as a Postdoctoral Associate in July of 2002, where he currently works with Dr. Ferreira on the stereoselective synthesis of flavanoid precursors, the semisynthesis of proanthocyanidin oligomers, and characterization of the proanthocyanidin profiles of selected transgenic plants.